Supplementary Material

Generation and reversible cyclisation of furfurylic radicals

Wilfred J. M. Lewis, Elizabeth J. Rayment, and Jeremy Robertson*

Department of Chemistry, University of Oxford, Chemistry Research Laboratory, Mansfield Road, Oxford, OX1 3TA, United Kingdom
Email: jeremy.robertson@chem.ox.ac.uk

Table of Contents

^{1}H and ^{13}C NMR data S2
Figure S1 ^{1}H–^{1}H NOESY (500 MHz, C_6D_6) spectrum of compound **22** S23
Figure S2 ^{1}H–^{1}H NOESY (500 MHz, C_6D_6) spectrum of compound **32** S24
DFT calculations S25

^{1}H NMR (500 MHz, $CDCl_3$)

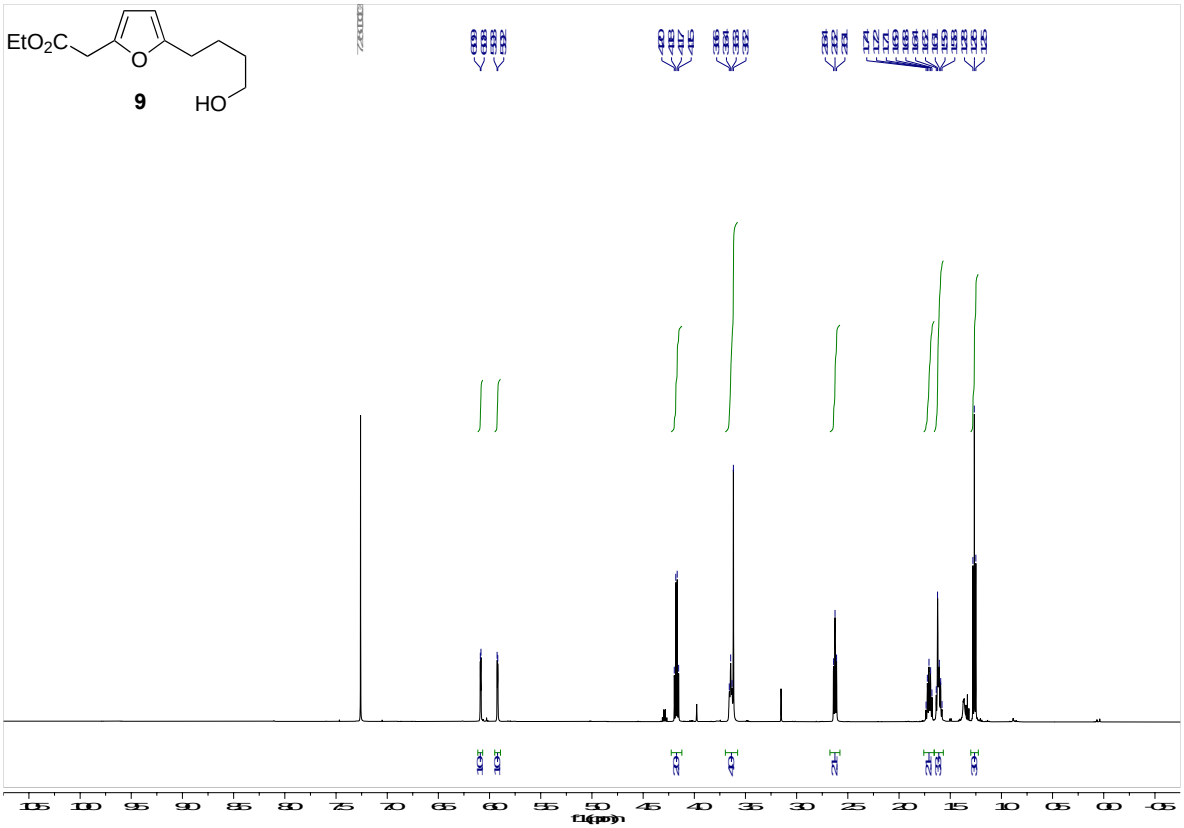

^{13}C NMR (126 MHz, $CDCl_3$)

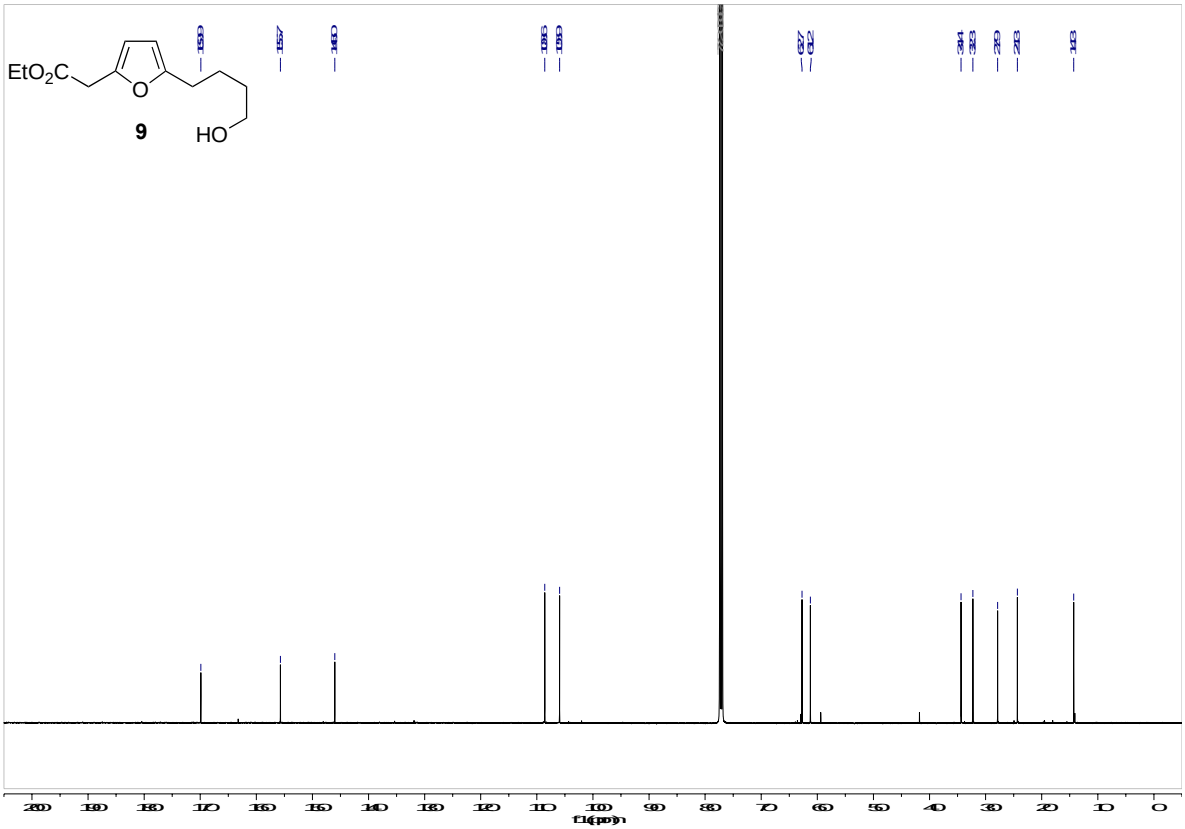

^{1}H NMR (400 MHz, $CDCl_3$)

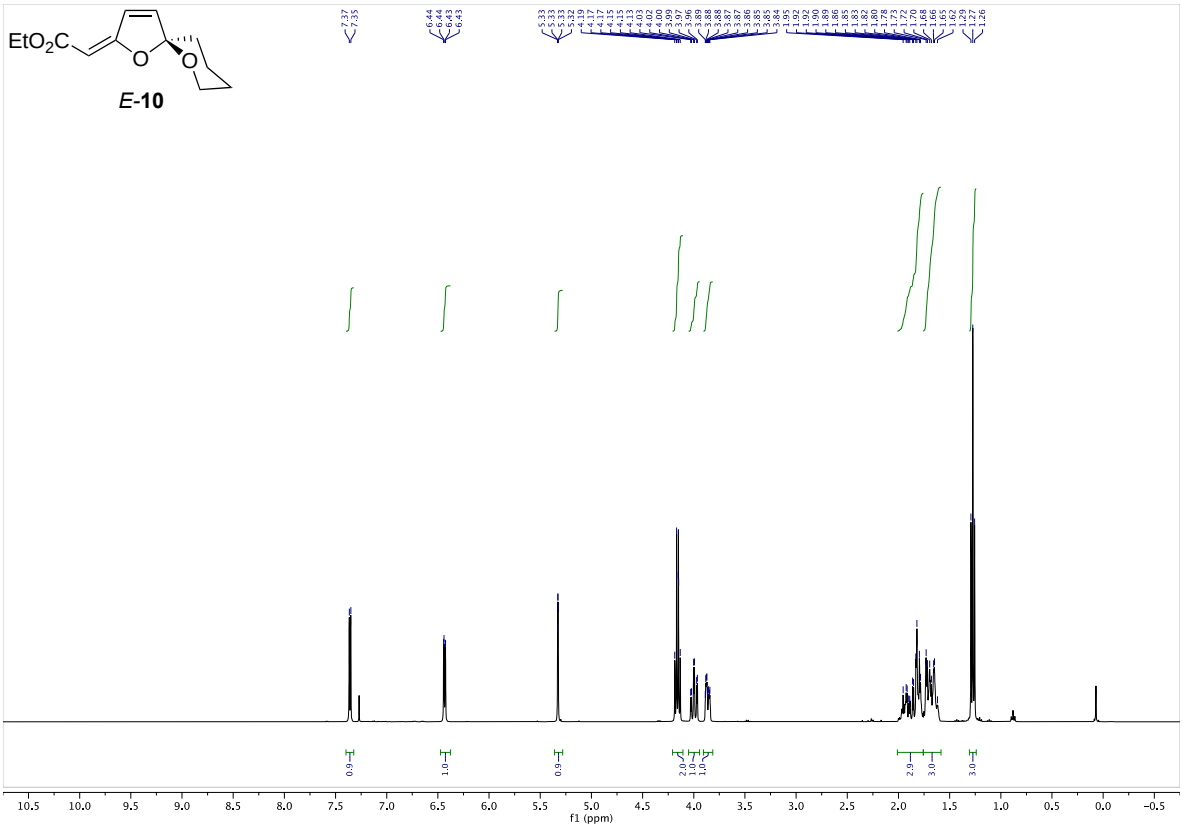

^{13}C NMR (101 MHz, $CDCl_3$)

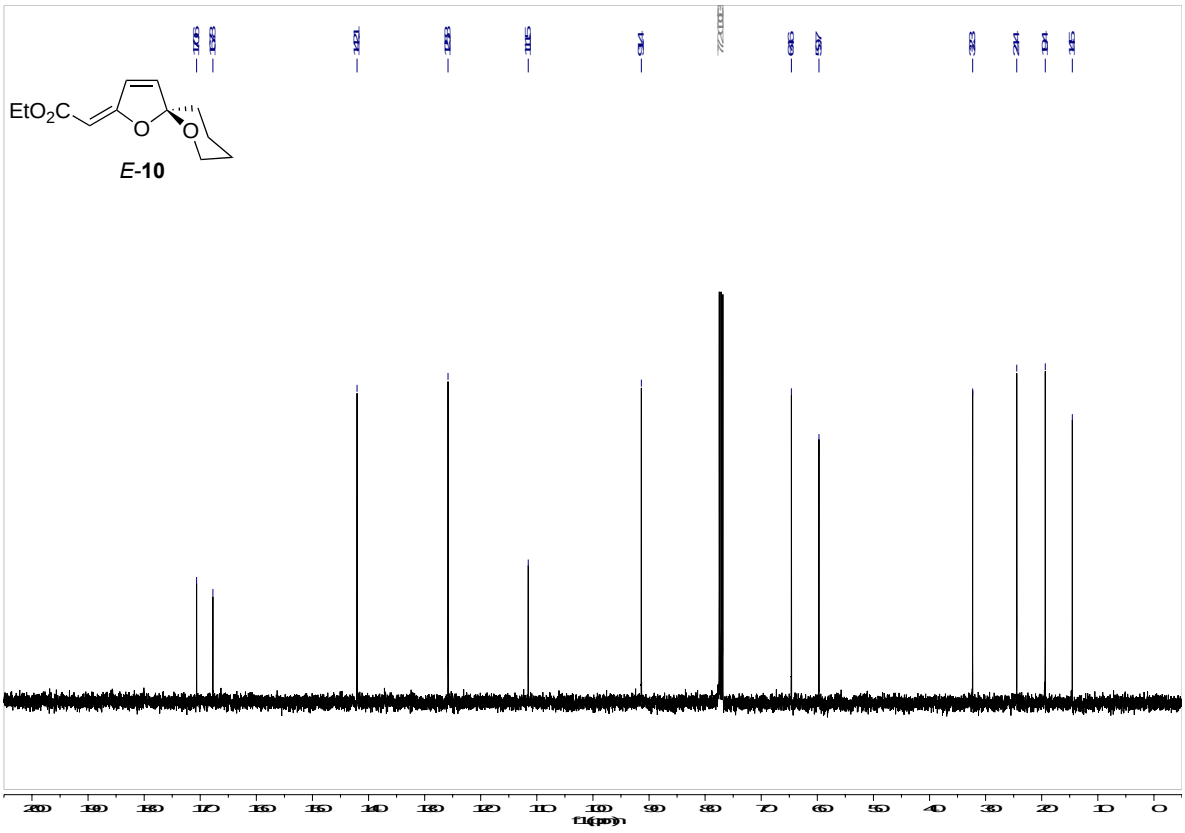

^{1}H NMR (400 MHz, $CDCl_3$)

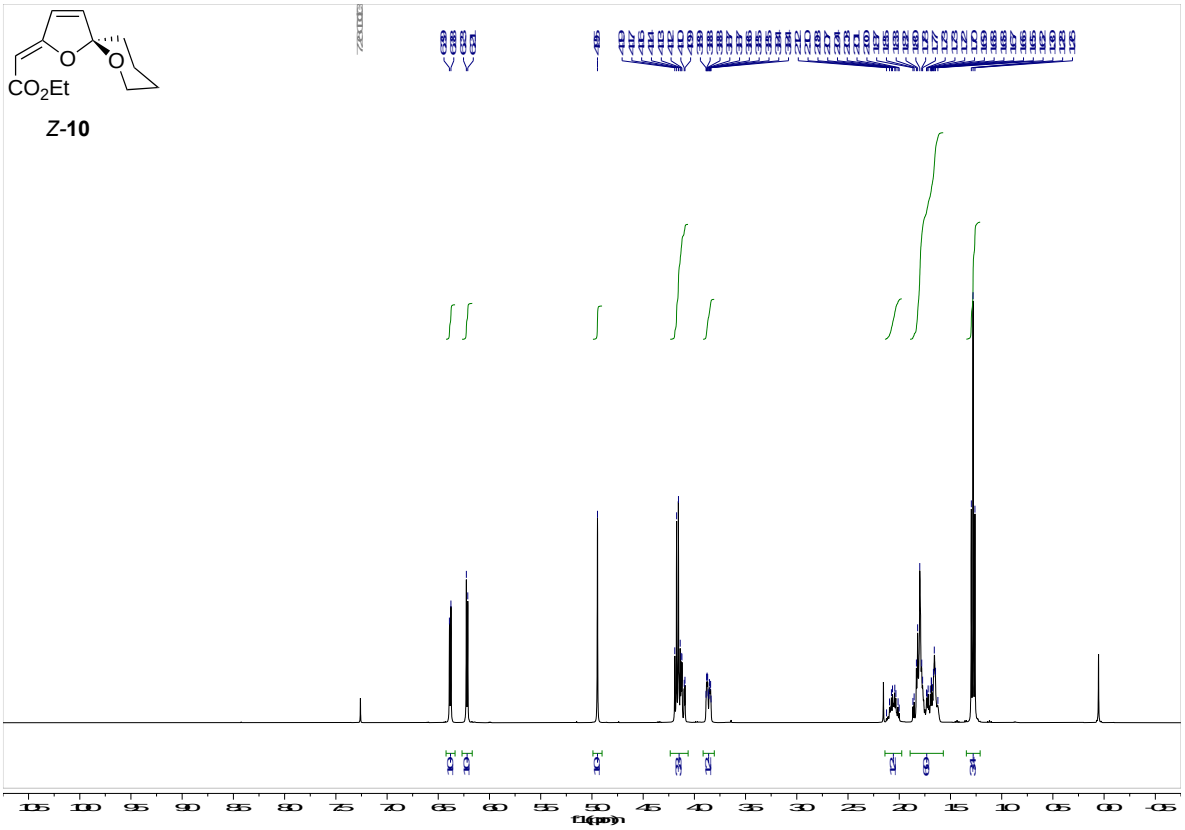

^{13}C NMR (101 MHz, $CDCl_3$)

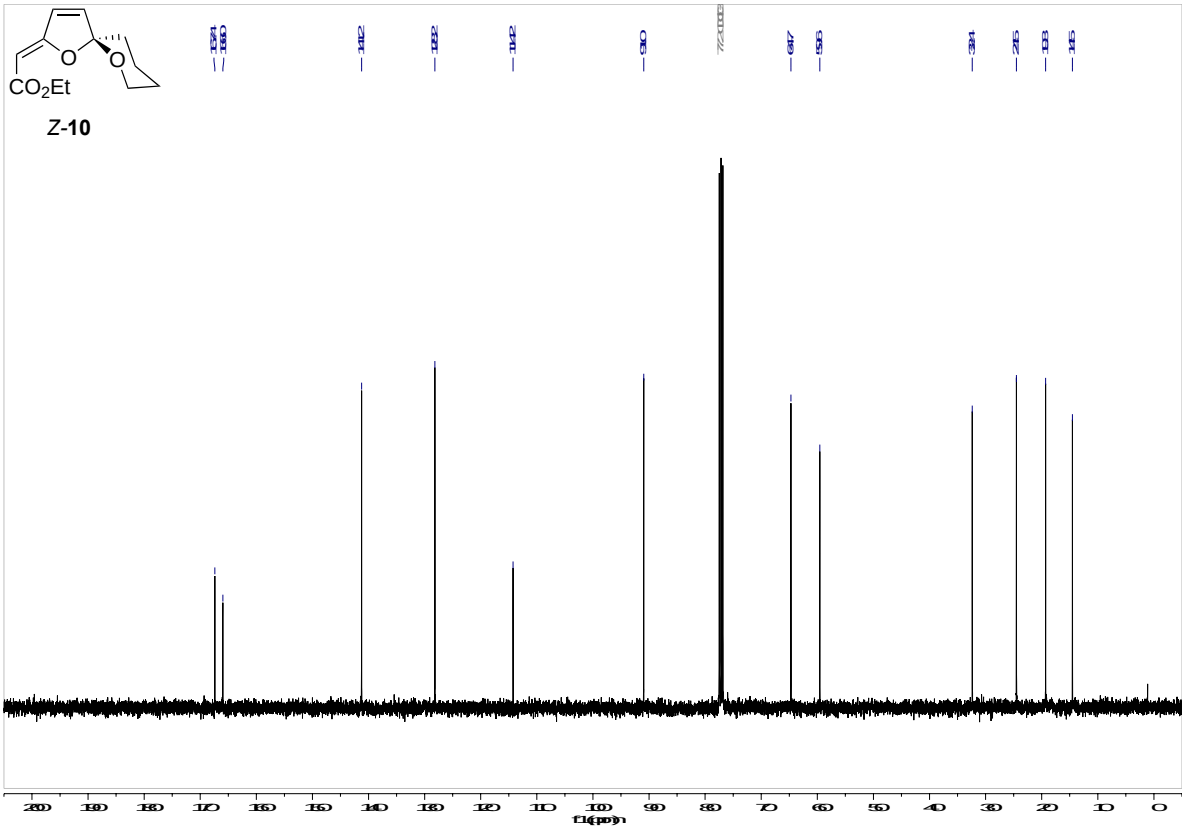

^{1}H NMR (400 MHz, $CDCl_3$)

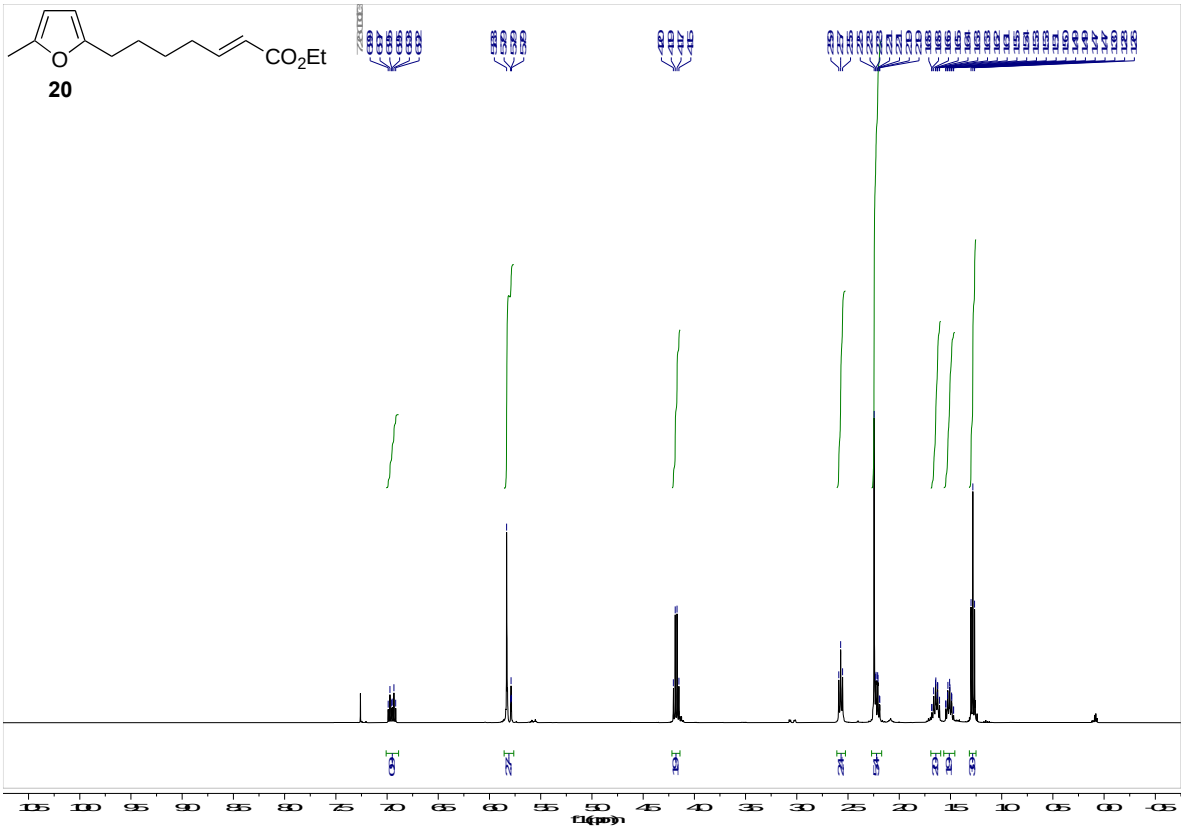

^{13}C NMR (101 MHz, $CDCl_3$)

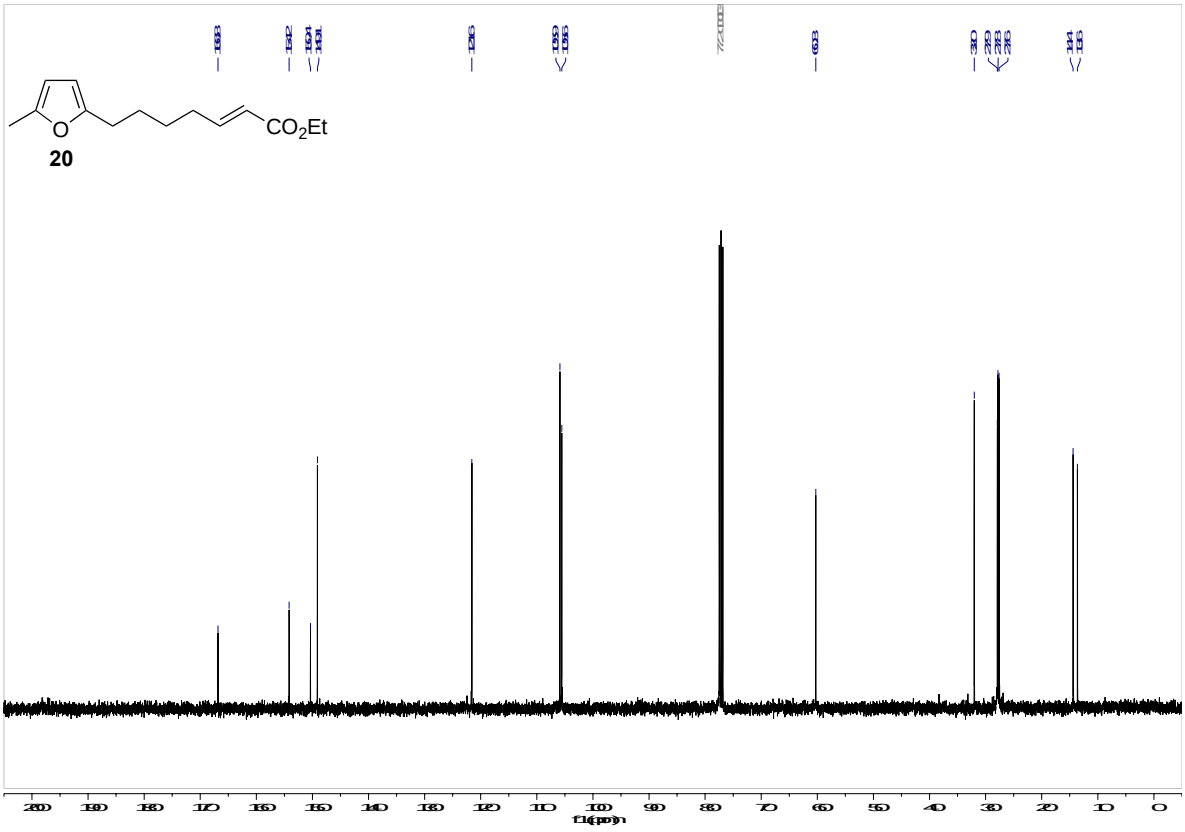

^{1}H NMR (400 MHz, $CDCl_3$)

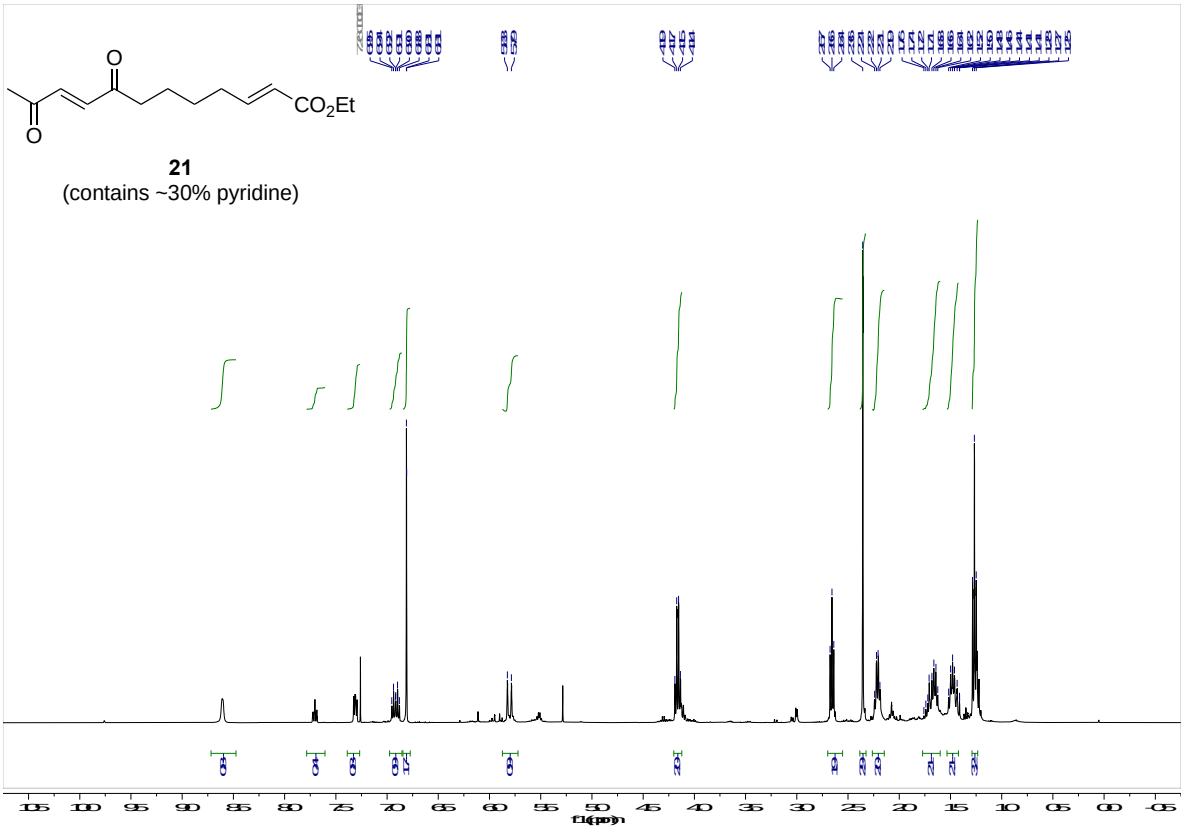

21
(contains ~30% pyridine)

^{13}C NMR (101 MHz, $CDCl_3$)

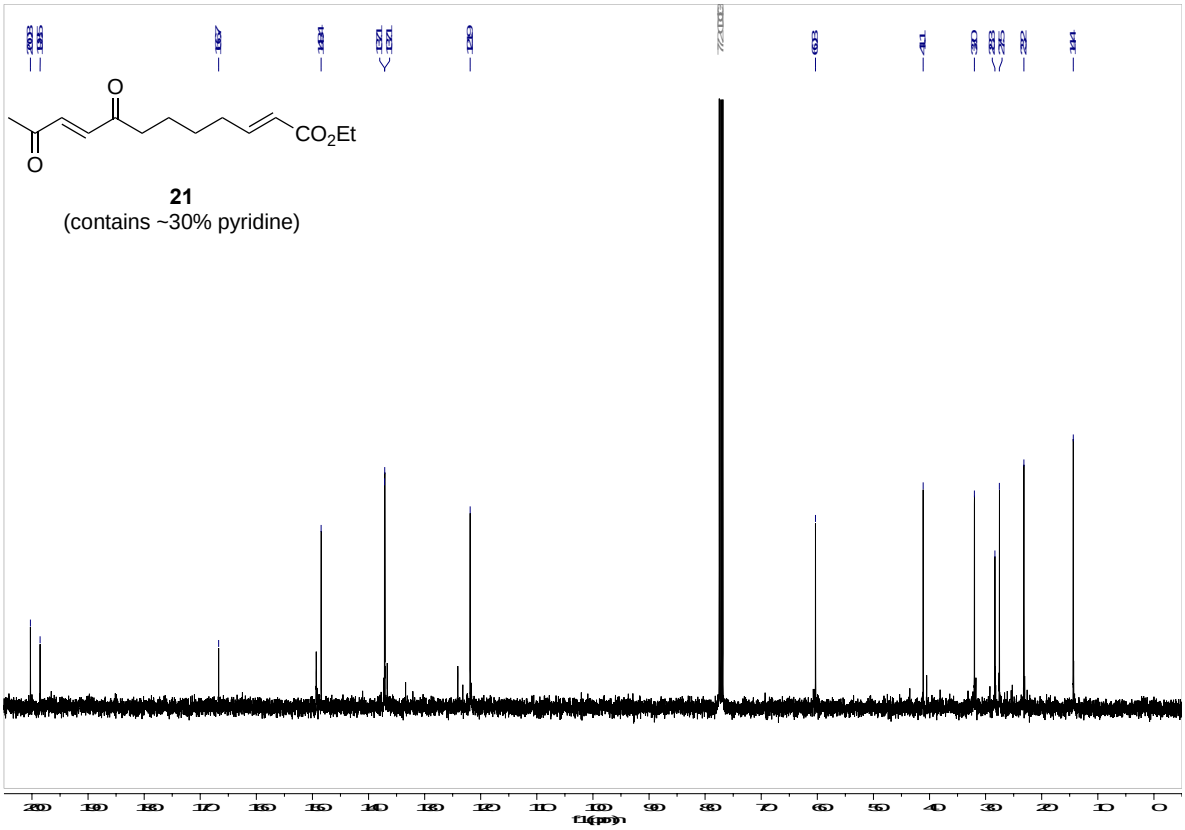

21
(contains ~30% pyridine)

^{1}H NMR (400 MHz, $CDCl_3$)

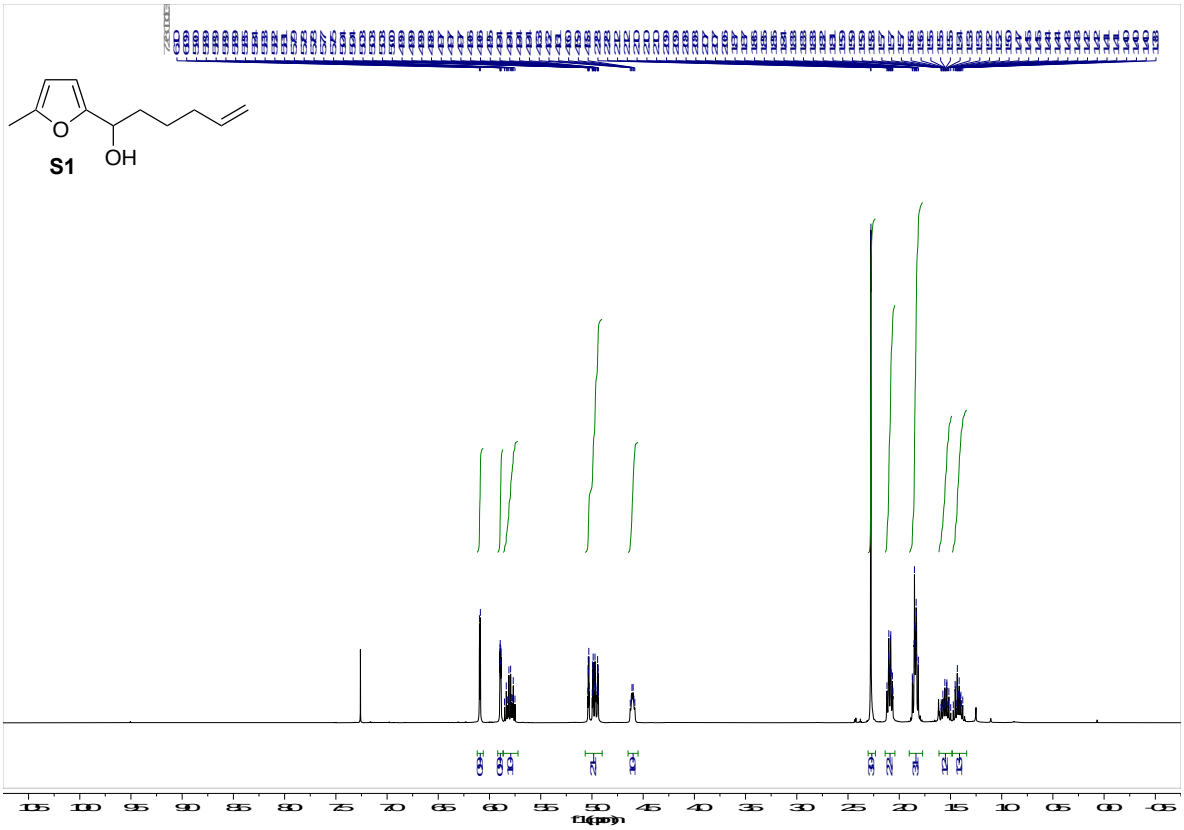

^{13}C NMR (101 MHz, $CDCl_3$)

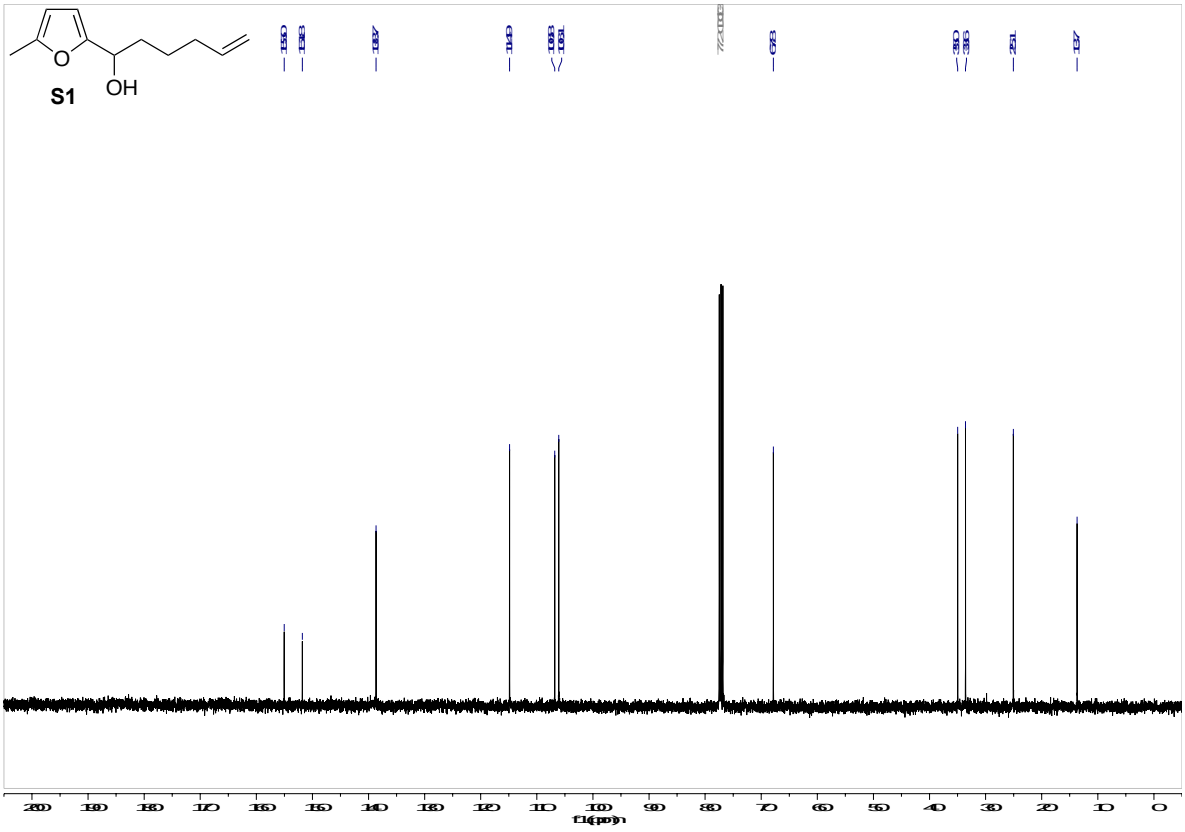

^{1}H NMR (400 MHz, $CDCl_3$)

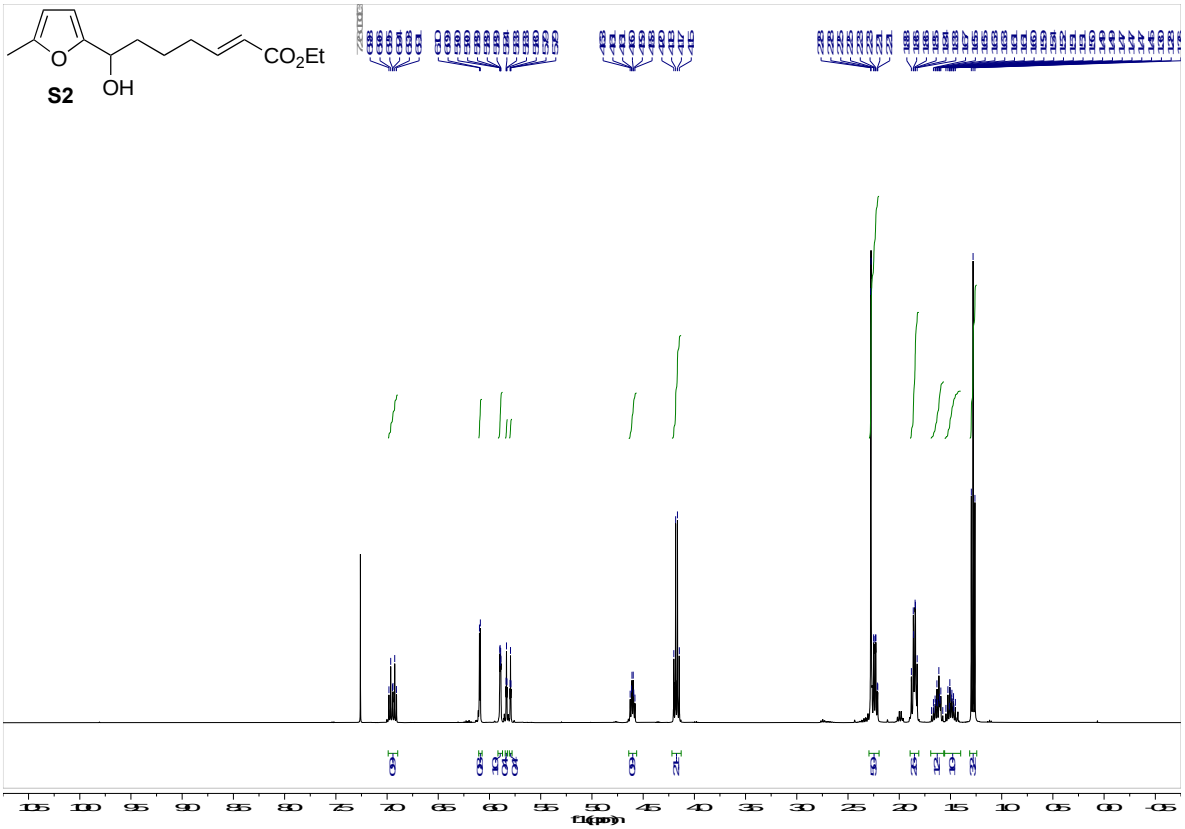

^{13}C NMR (101 MHz, $CDCl_3$)

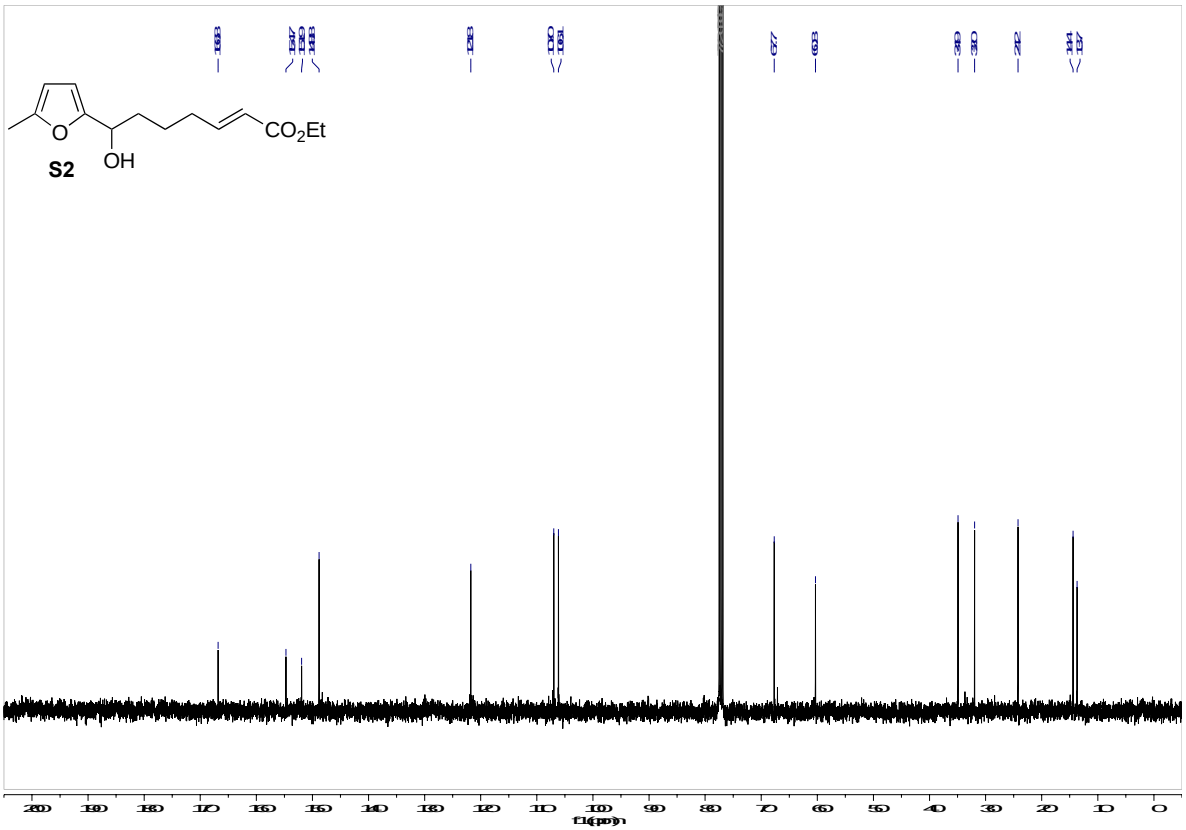

^{1}H NMR (500 MHz, C_6D_6)

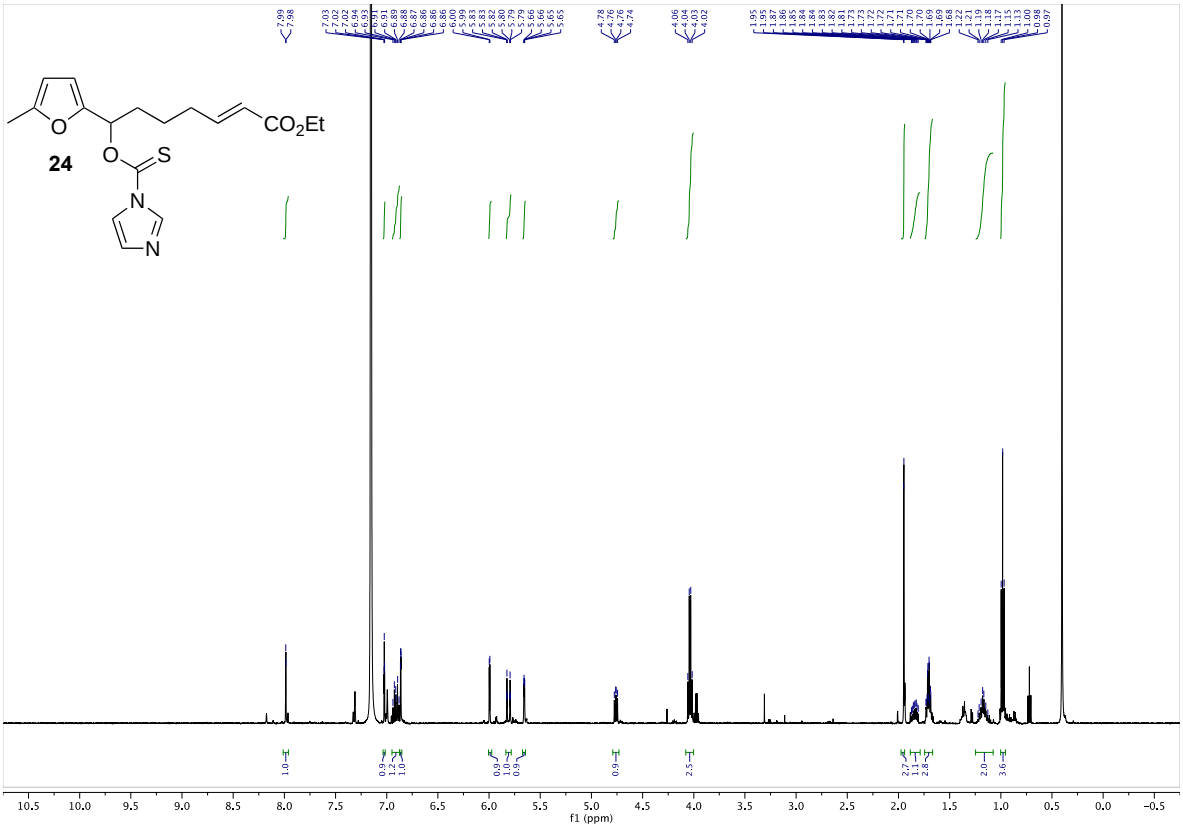

^{13}C NMR (126 MHz, C_6D_6)

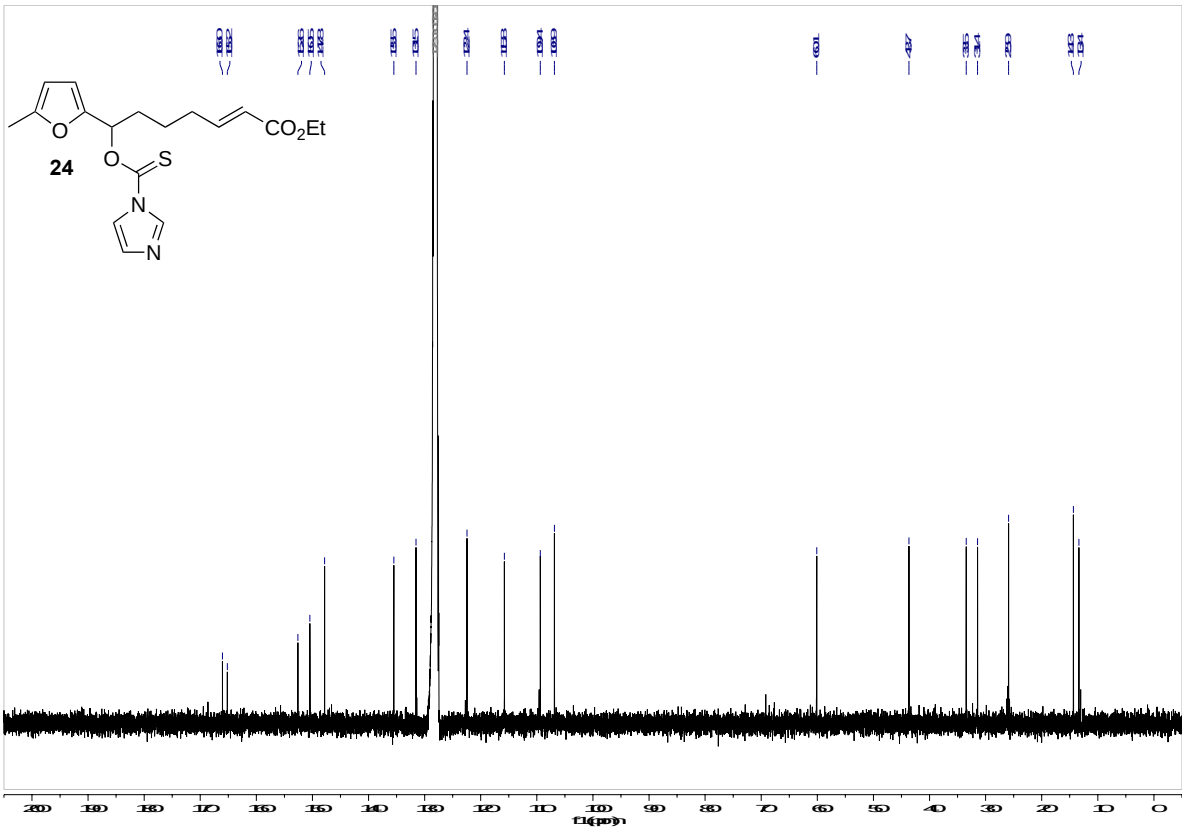

^{1}H NMR (500 MHz, C_6D_6)

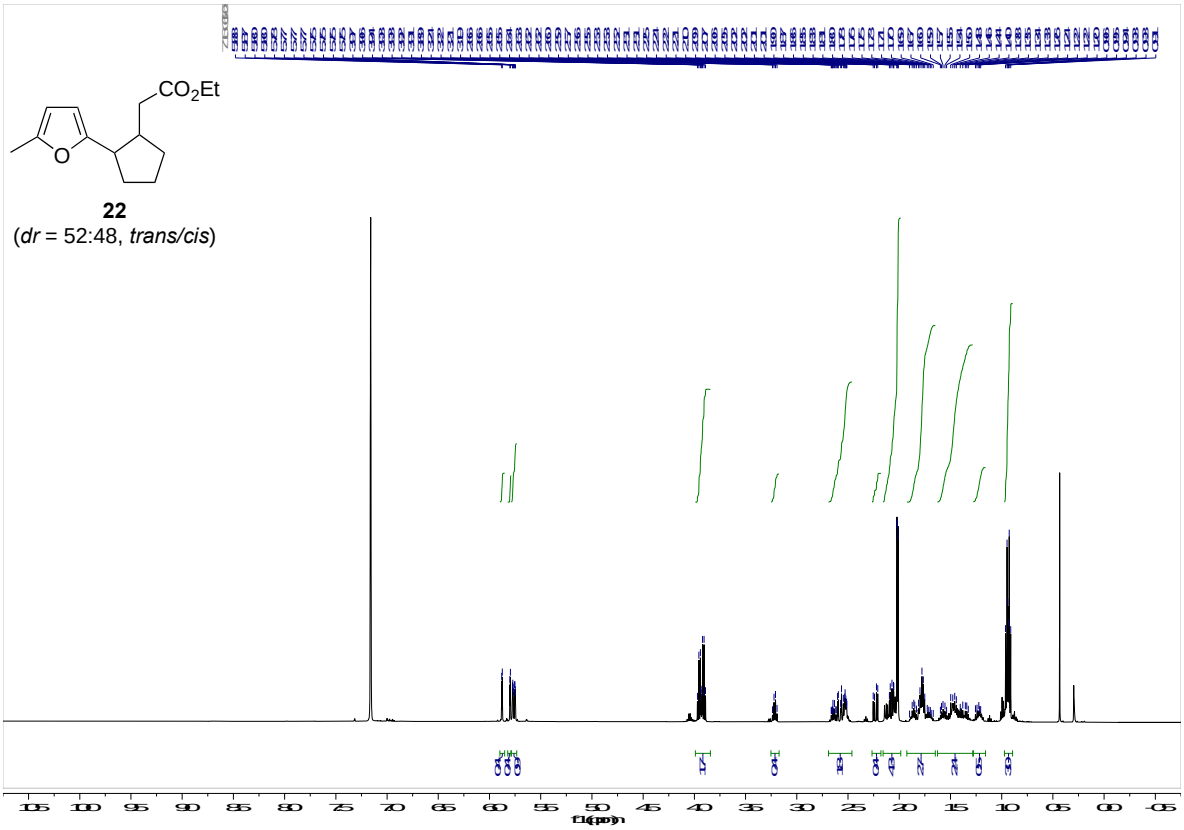

22
(*dr* = 52:48, *trans/cis*)

^{13}C NMR (126 MHz, C_6D_6)

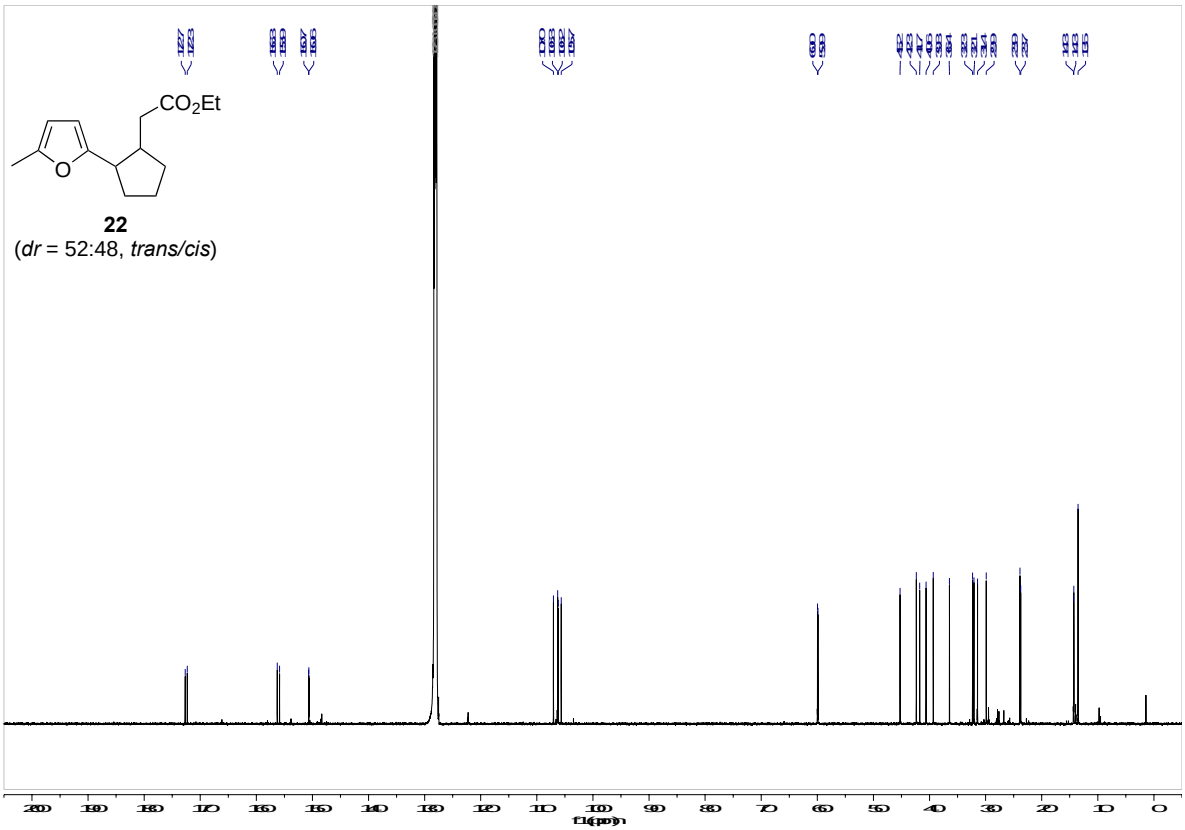

22
(*dr* = 52:48, *trans/cis*)

^{1}H NMR (400 MHz, $CDCl_3$)

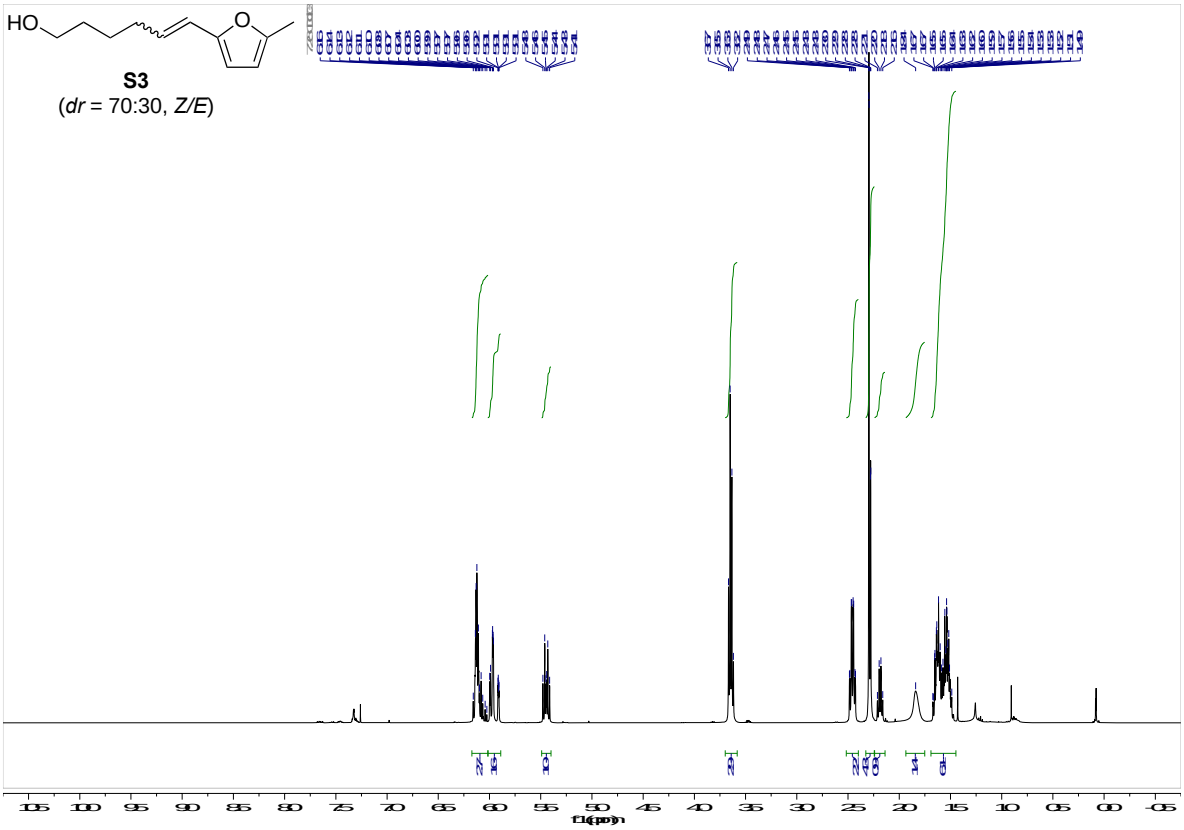

^{13}C NMR (101 MHz, $CDCl_3$)

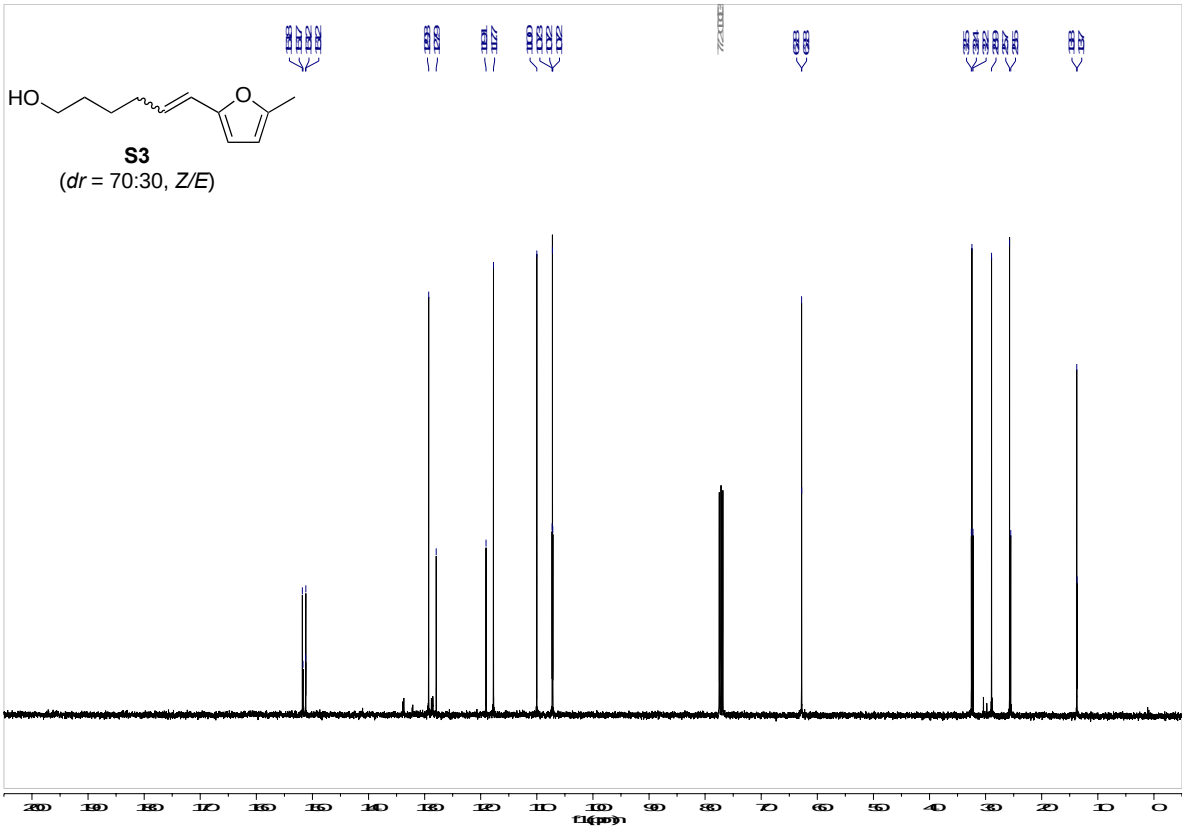

^{1}H NMR (500 MHz, C_6D_6)

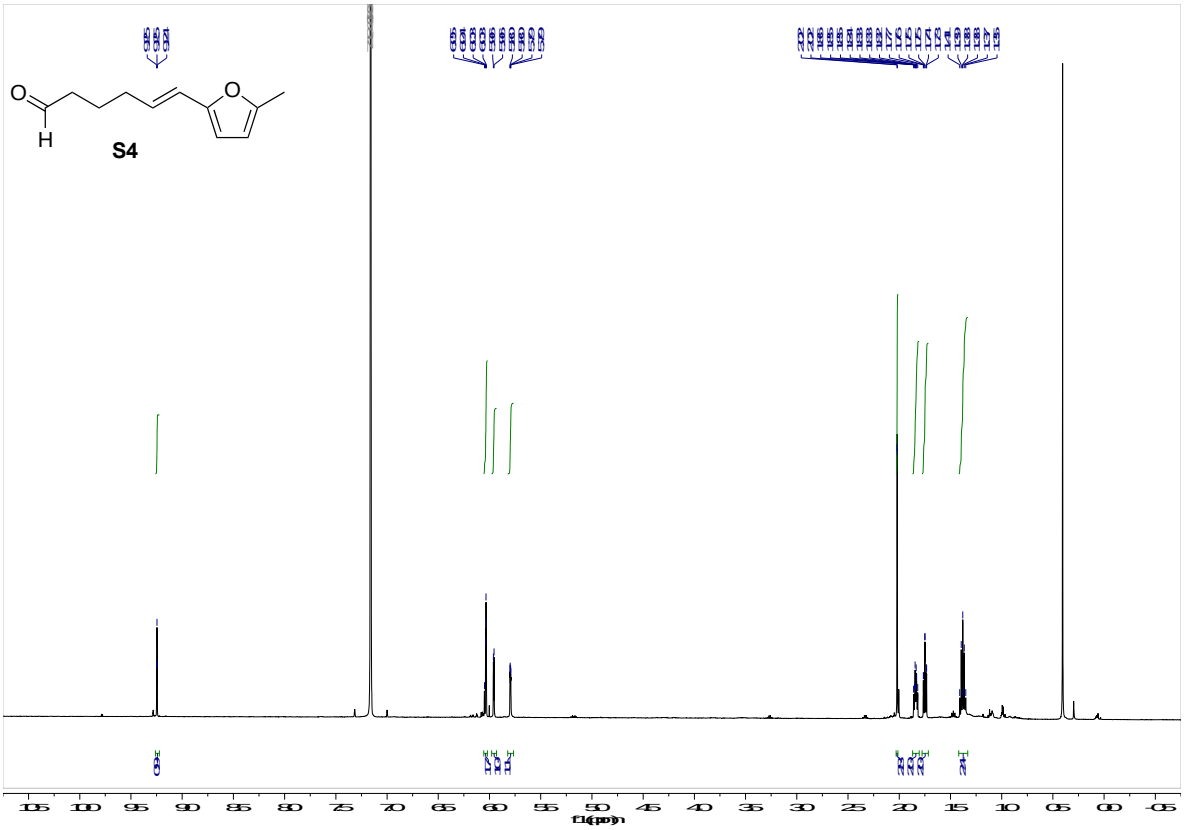

^{13}C NMR (126 MHz, C_6D_6)

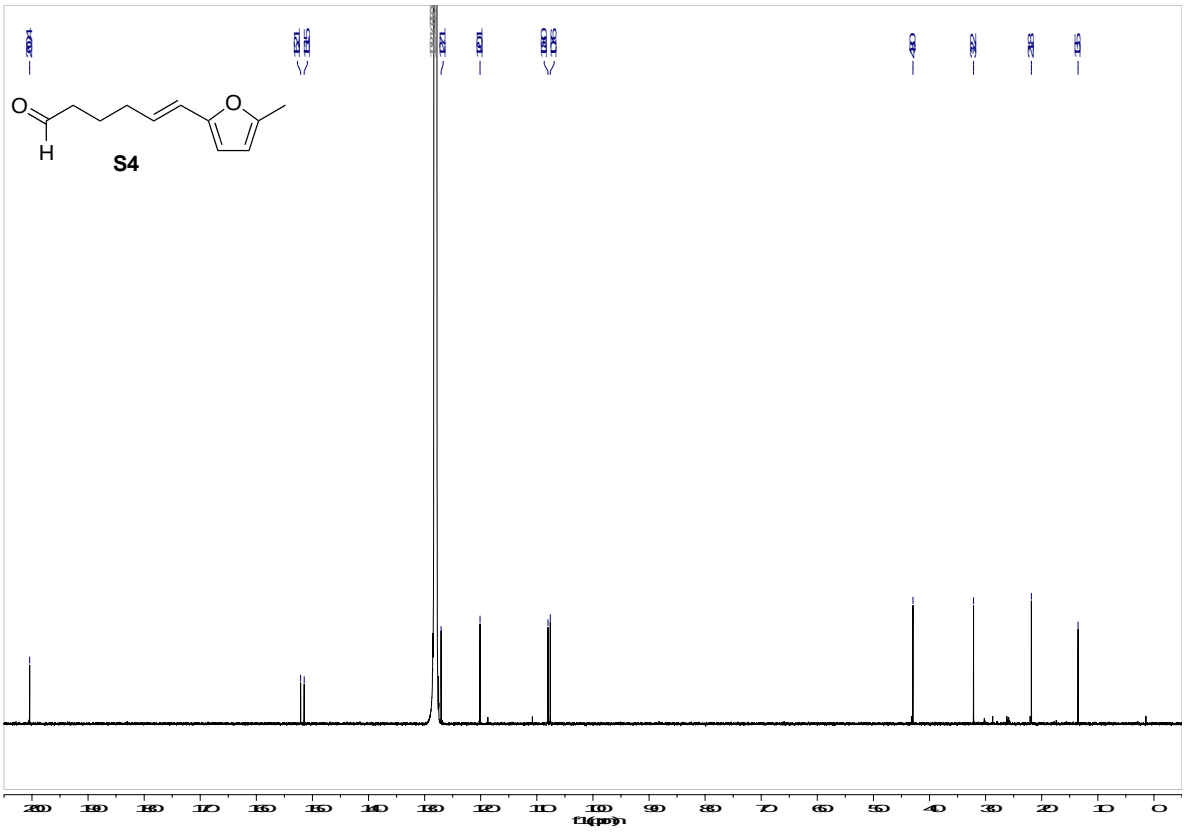

^{1}H NMR (400 MHz, C_6D_6)

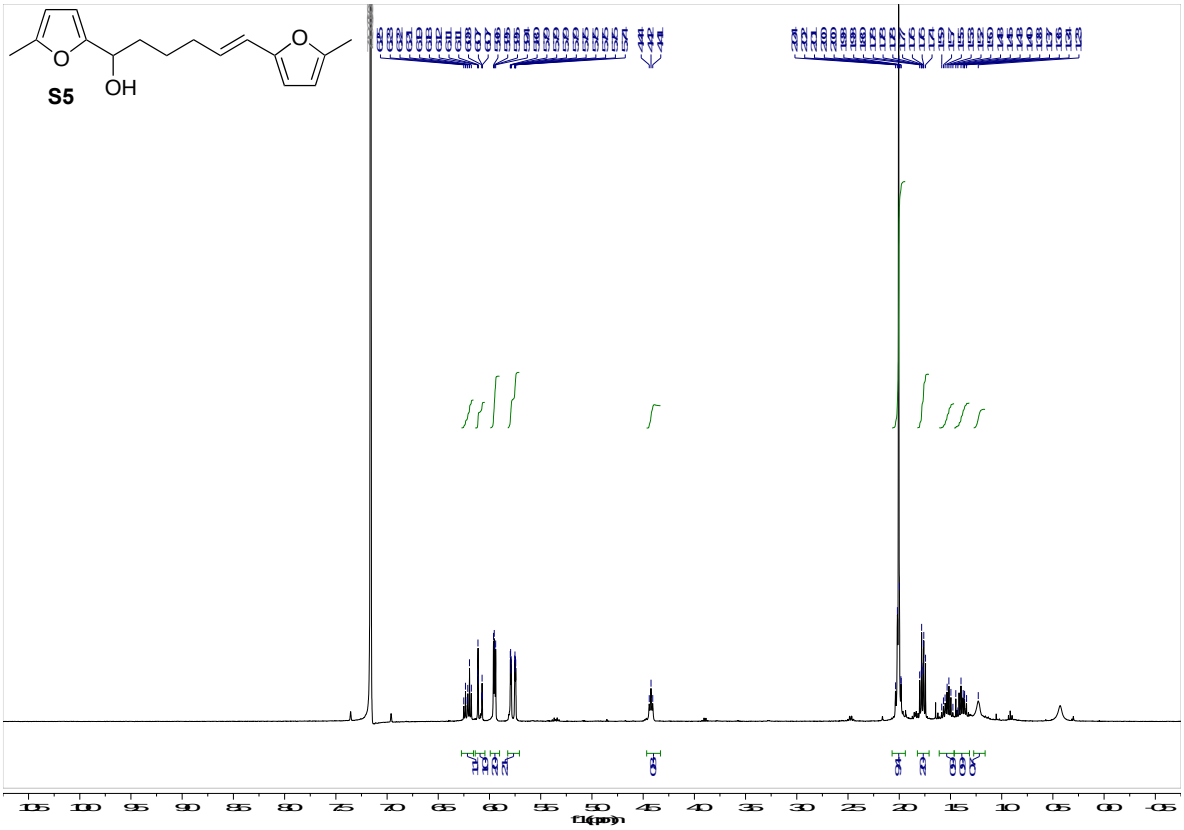

^{13}C NMR (101 MHz, C_6D_6)

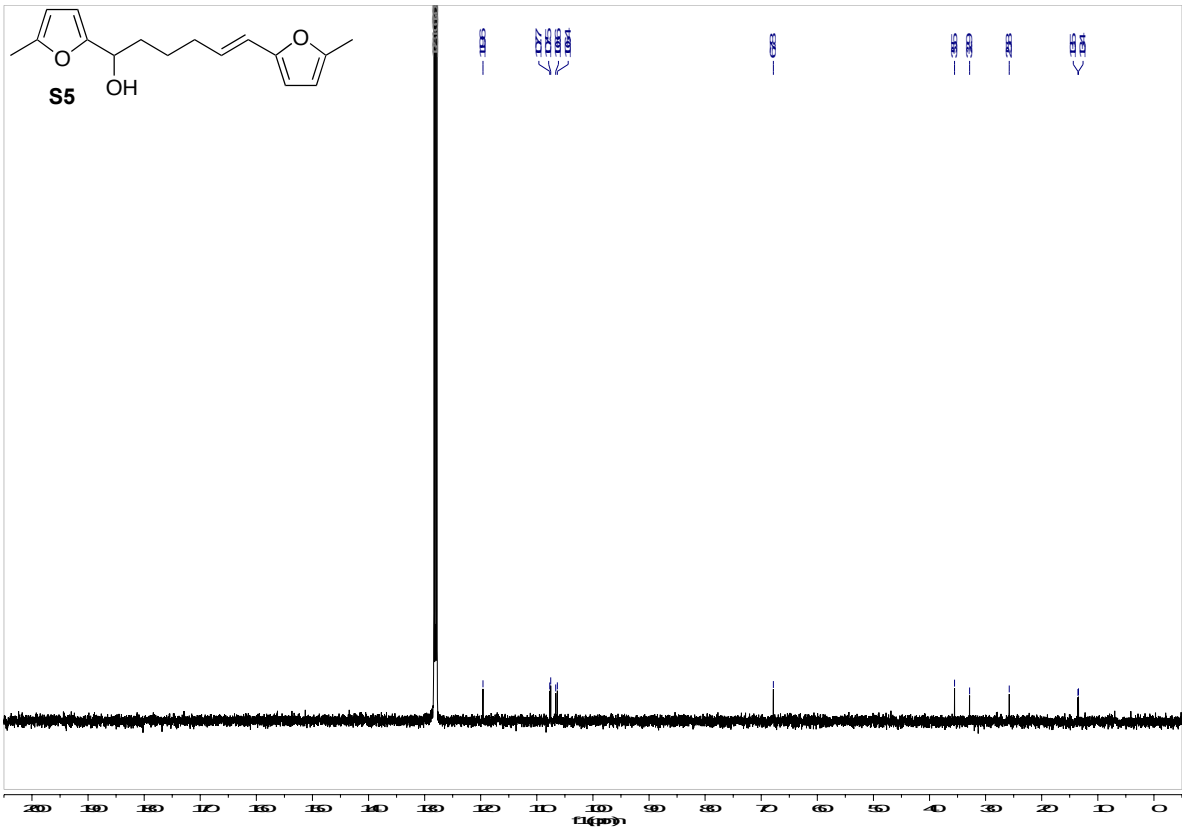

^{1}H NMR (400 MHz, C_6D_6)

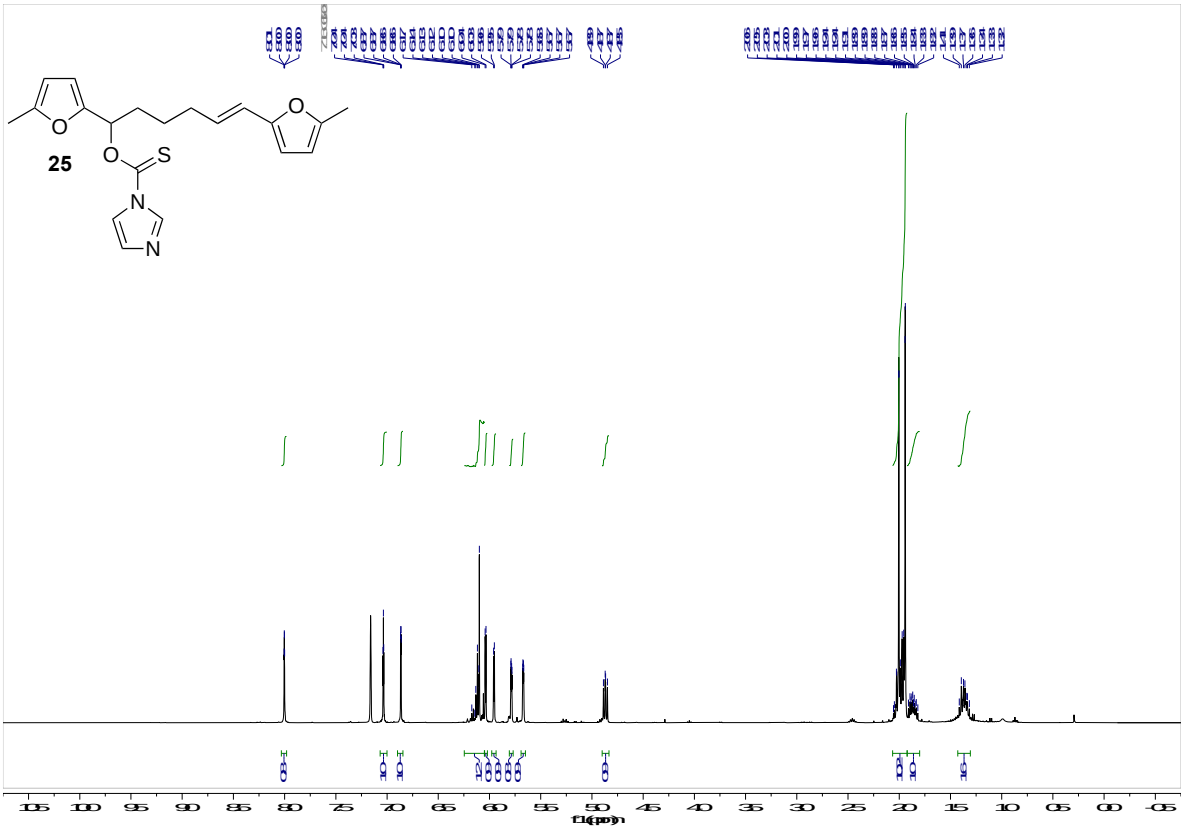

^{13}C NMR (101 MHz, C_6D_6)

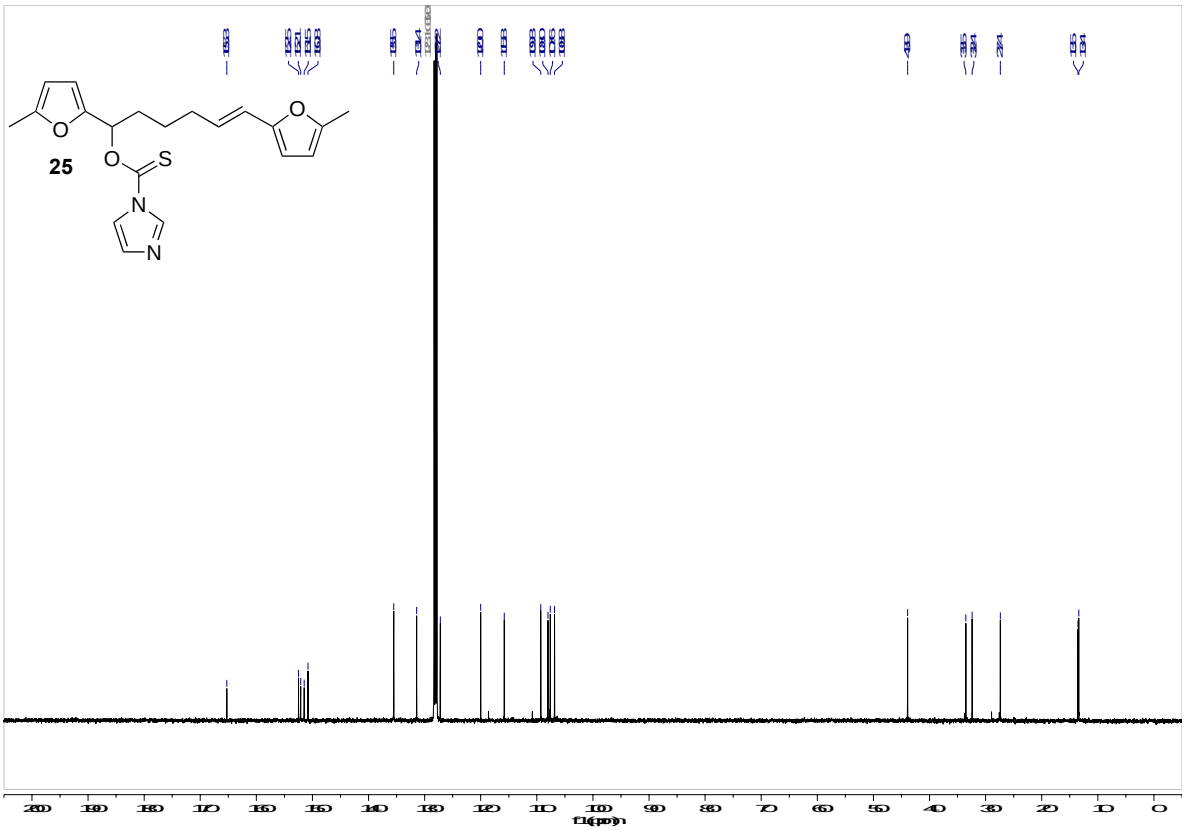

^{1}H NMR (400 MHz, C_6D_6)

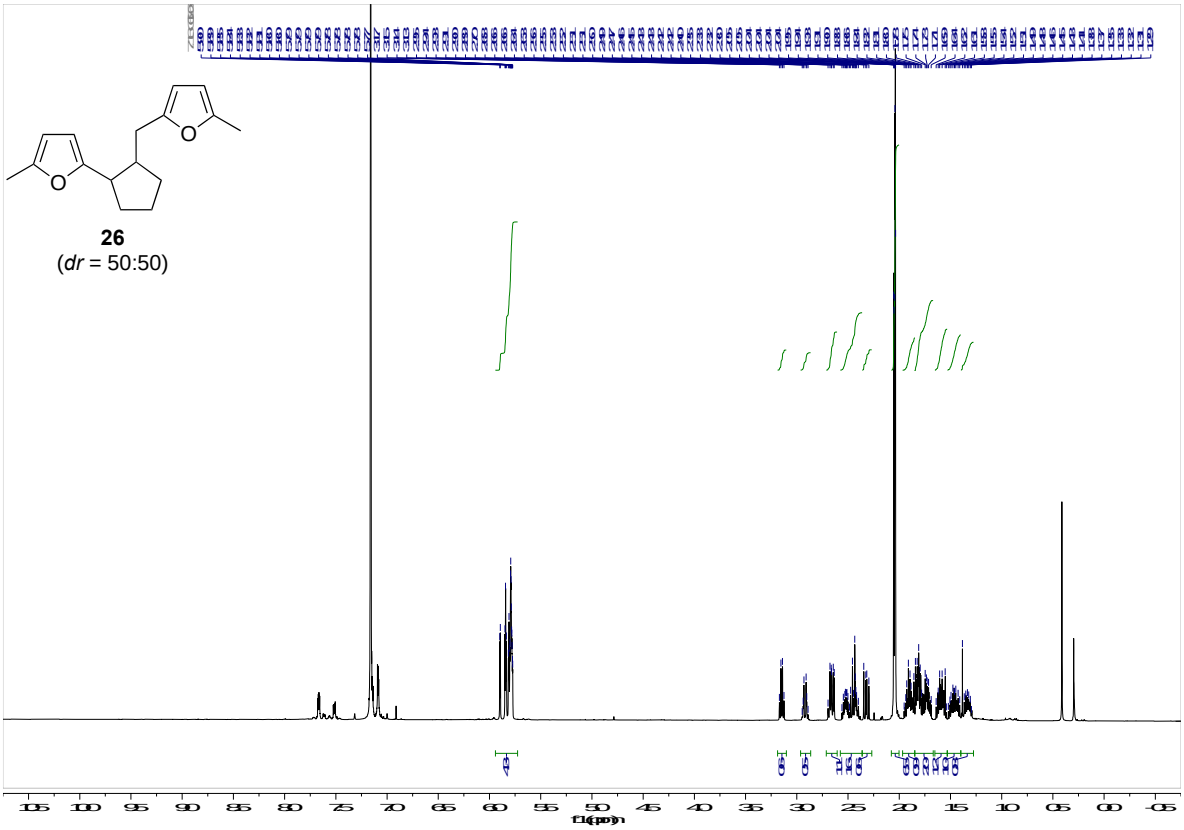

^{13}C NMR (101 MHz, C_6D_6)

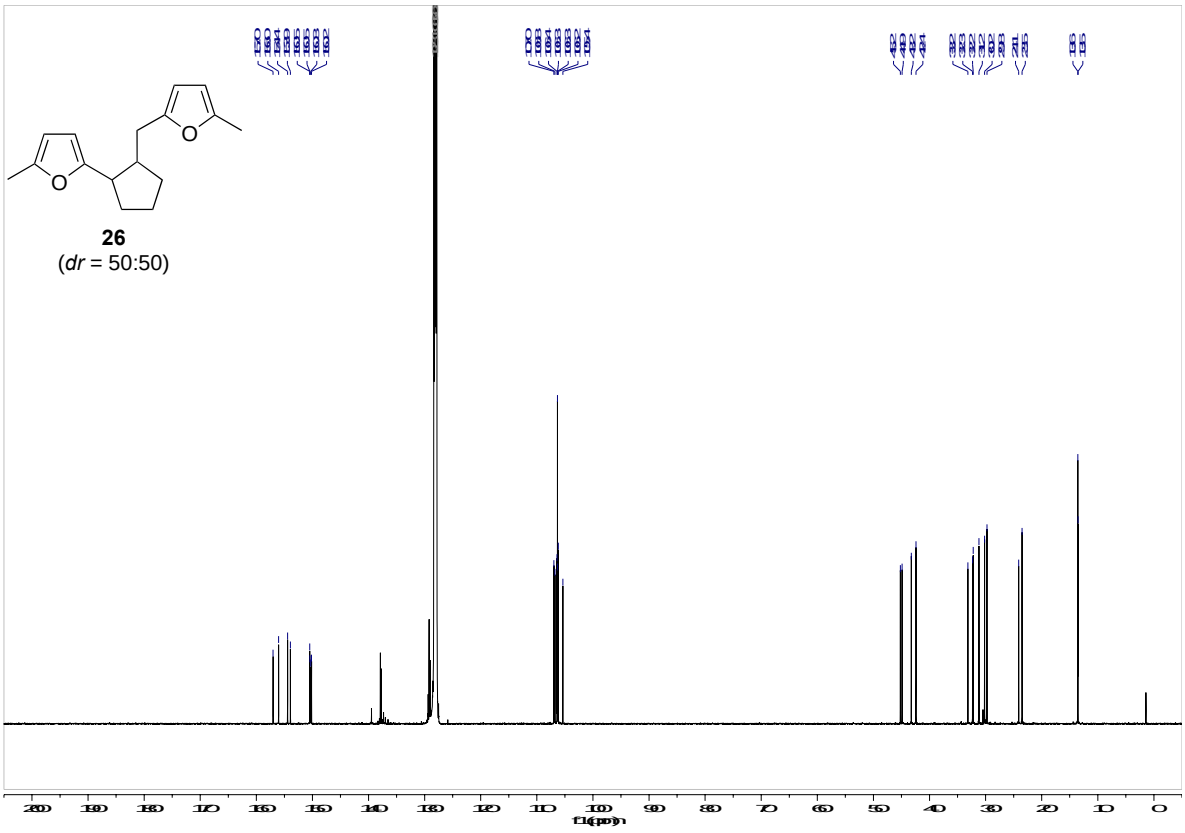

^{1}H NMR (400 MHz, $CDCl_3$)

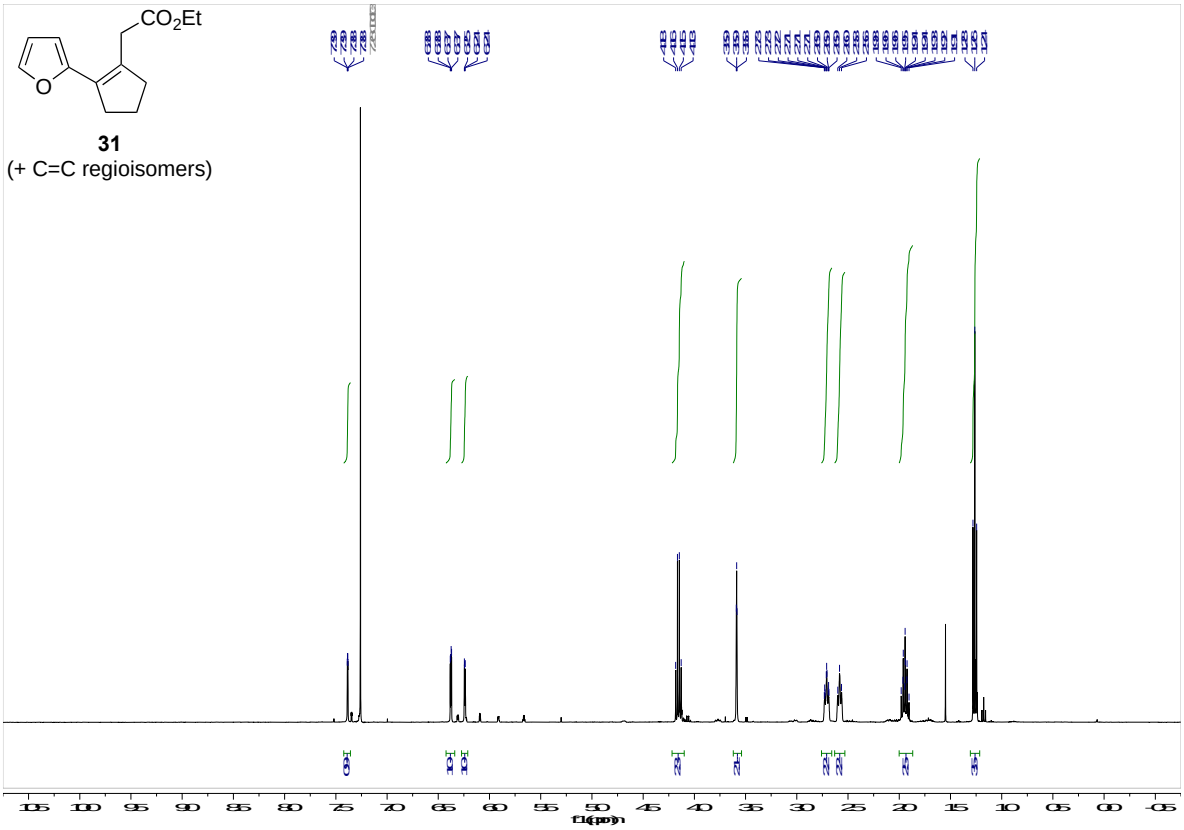

^{13}C NMR (101 MHz, $CDCl_3$)

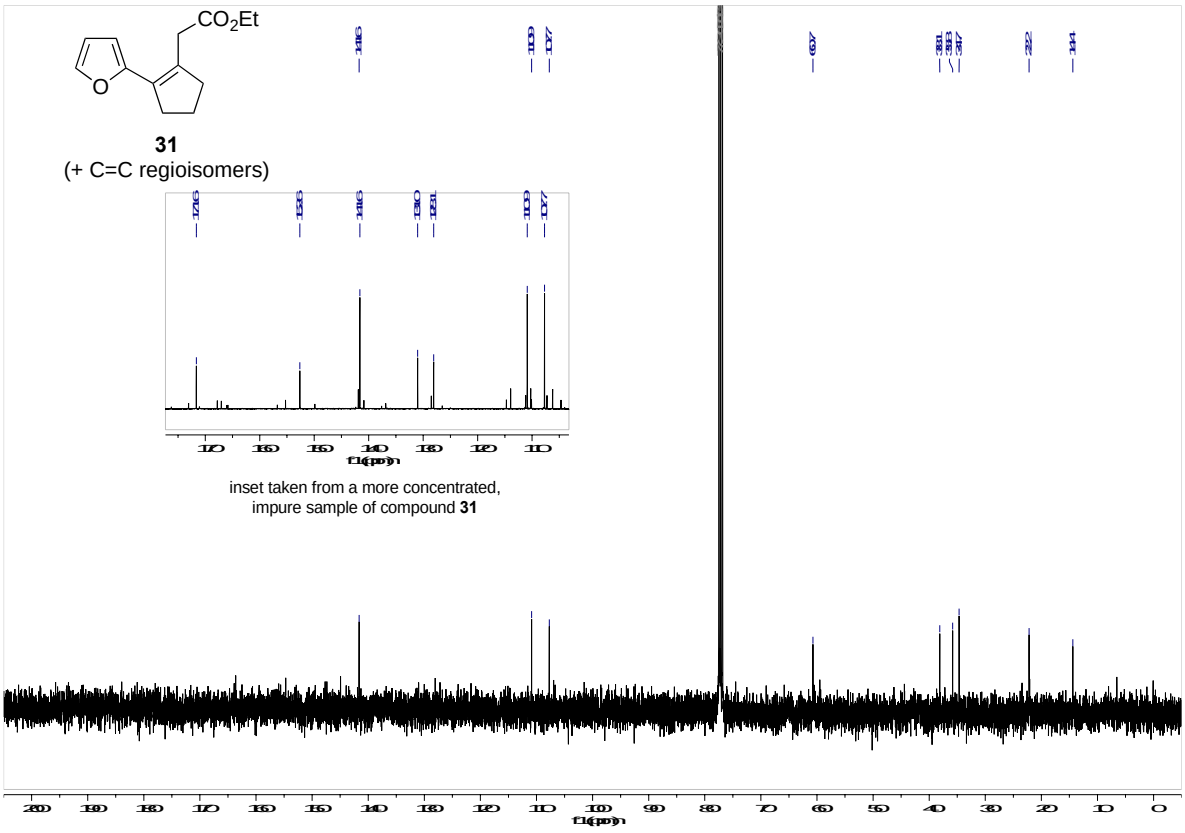

^{1}H NMR (500 MHz, C_6D_6)

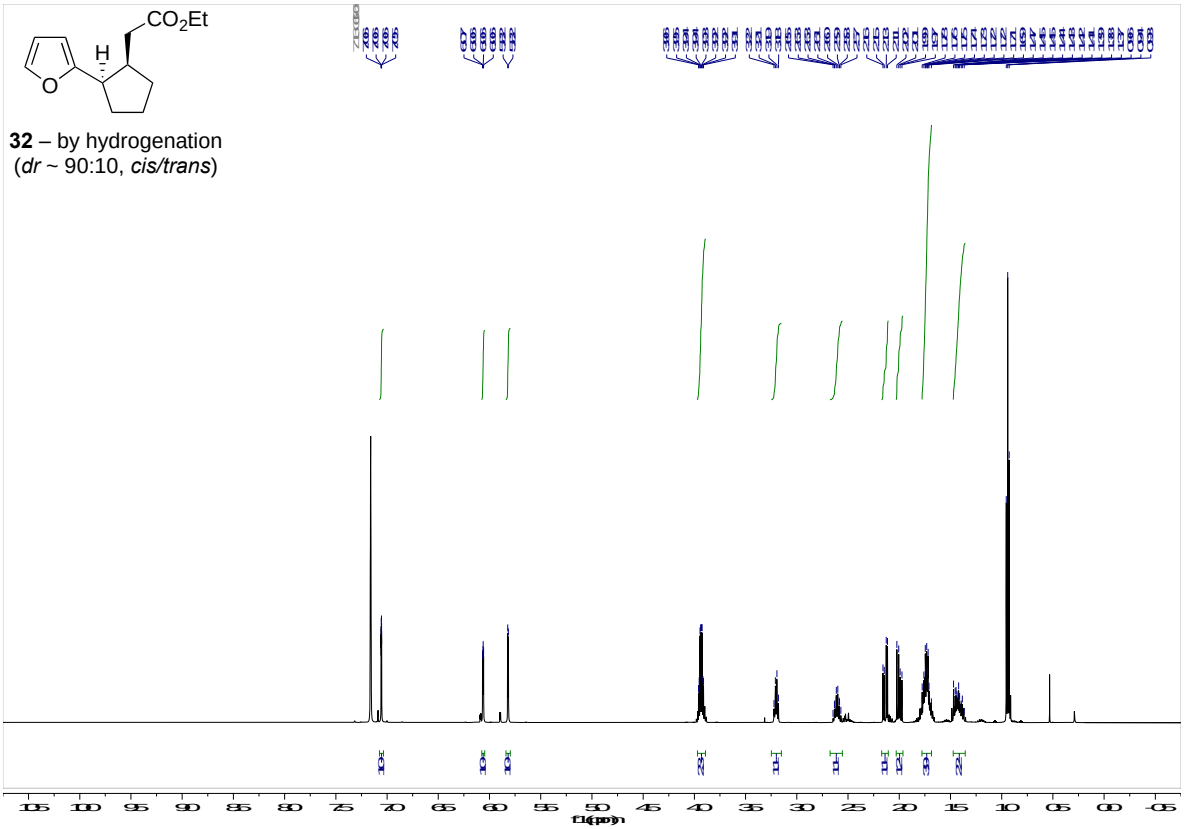

32 – by hydrogenation
(*dr* ~ 90:10, *cis/trans*)

^{13}C NMR (126 MHz, C_6D_6)

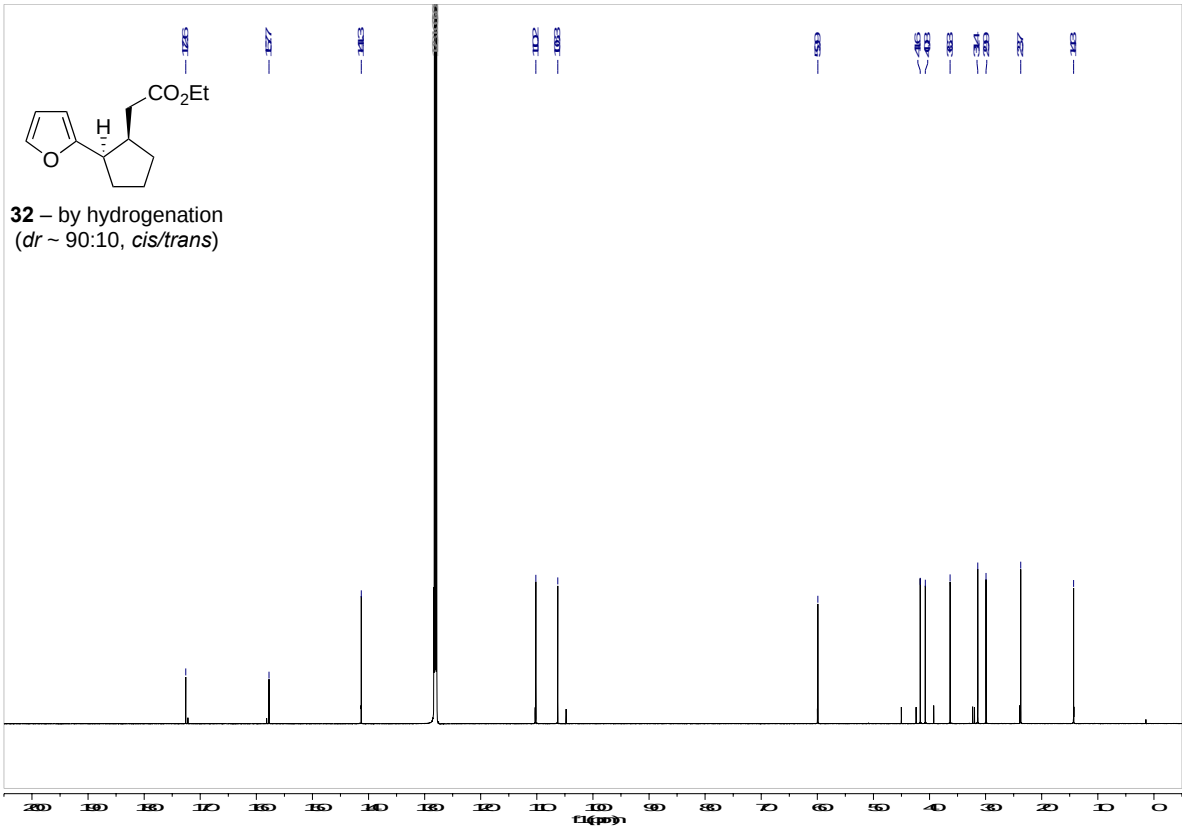

32 – by hydrogenation
(*dr* ~ 90:10, *cis/trans*)

^{1}H NMR (500 MHz, C_6D_6)

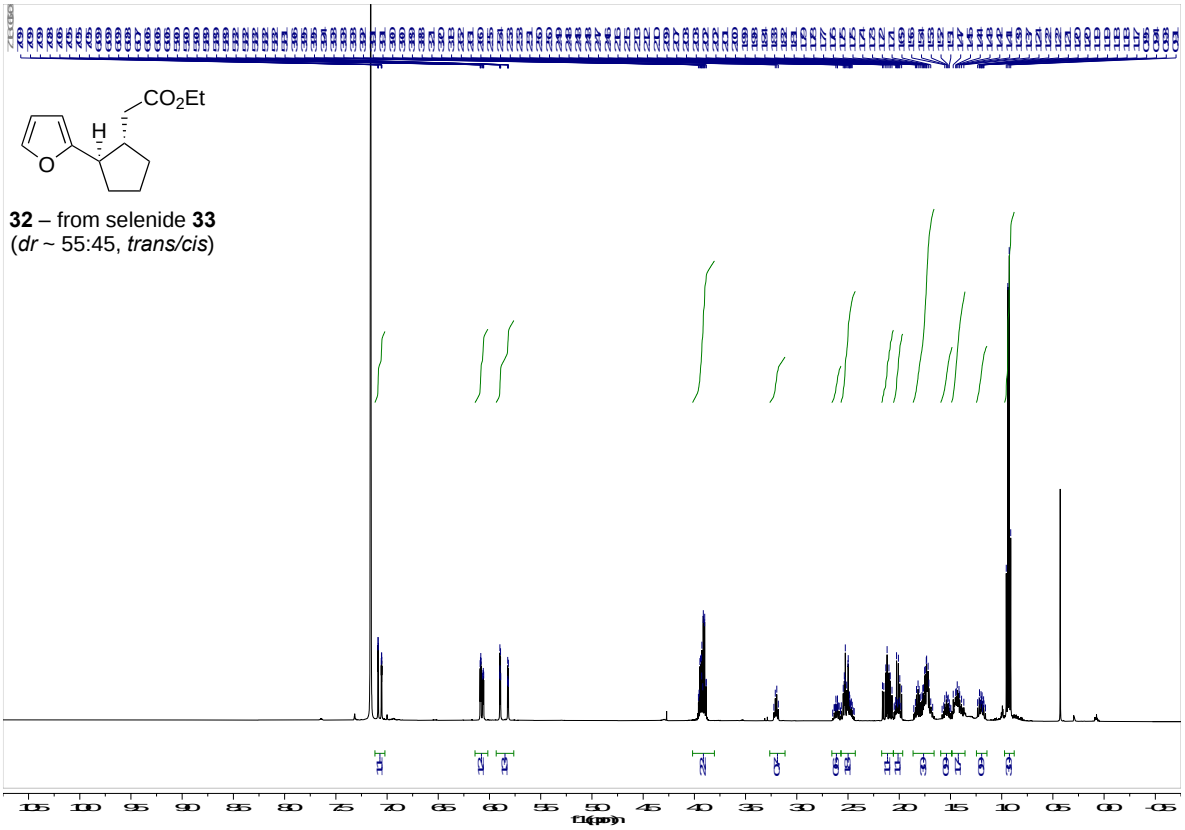

^{13}C NMR (126 MHz, C_6D_6)

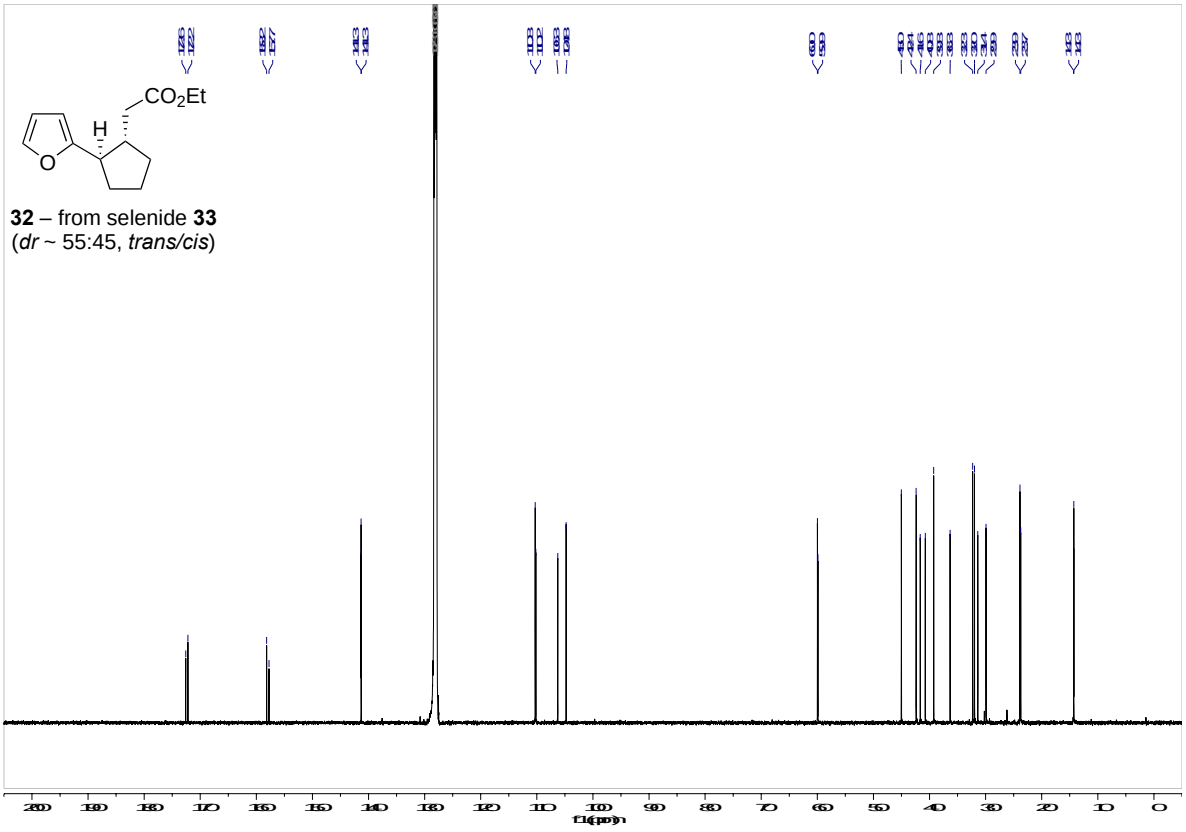

^{1}H NMR (400 MHz, C_6D_6)

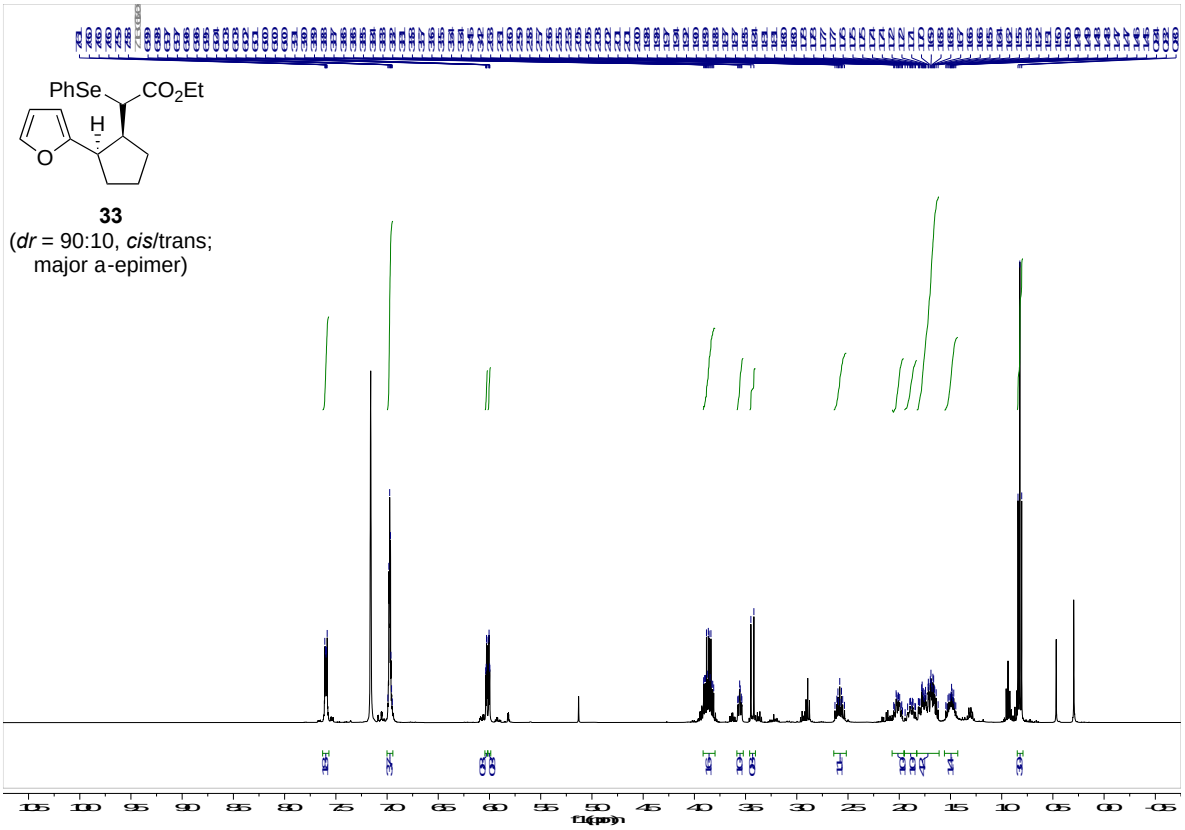

33
(*dr* = 90:10, *cis*/trans;
major a-epimer)

^{13}C NMR (101 MHz, C_6D_6)

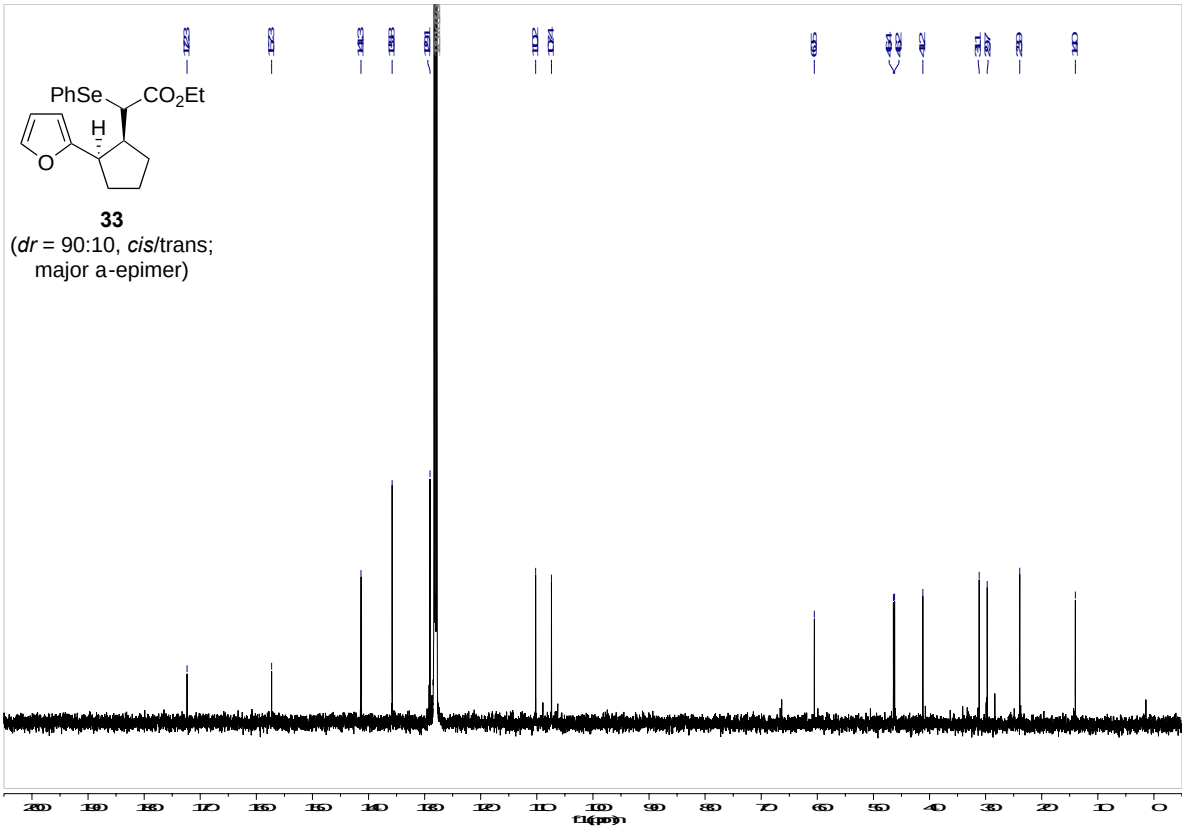

33
(*dr* = 90:10, *cis*/trans;
major a-epimer)

^{1}H NMR (400 MHz, C_6D_6)

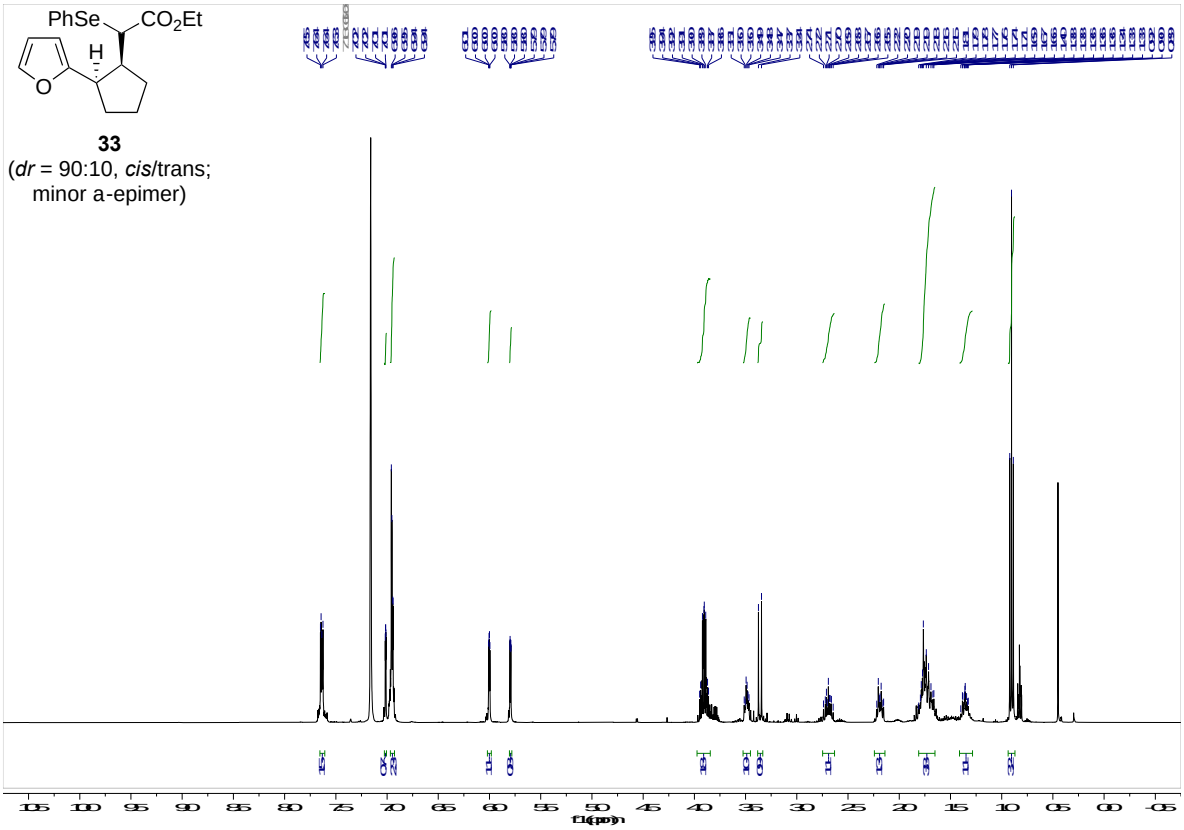

33
(*dr* = 90:10, *cis*/trans;
minor a-epimer)

^{13}C NMR (101 MHz, C_6D_6)

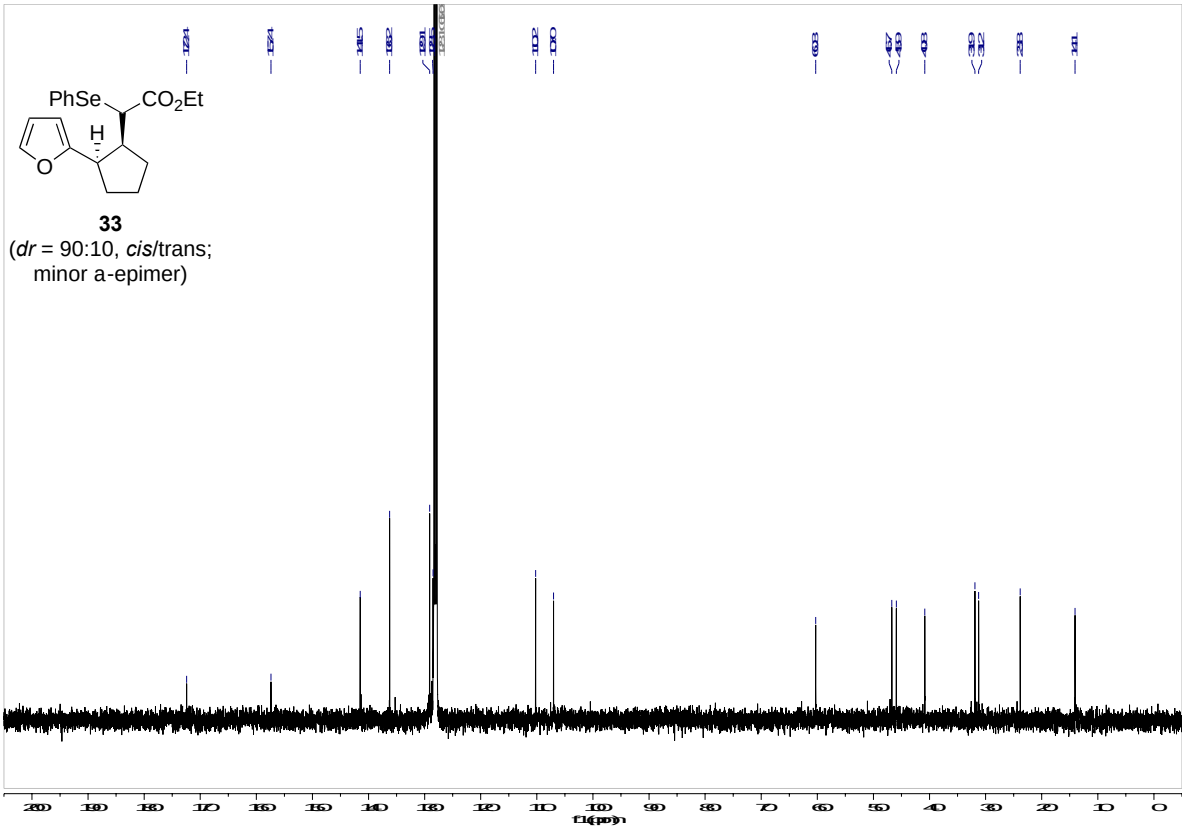

33
(*dr* = 90:10, *cis*/trans;
minor a-epimer)

^{1}H NMR (500 MHz, C_6D_6)

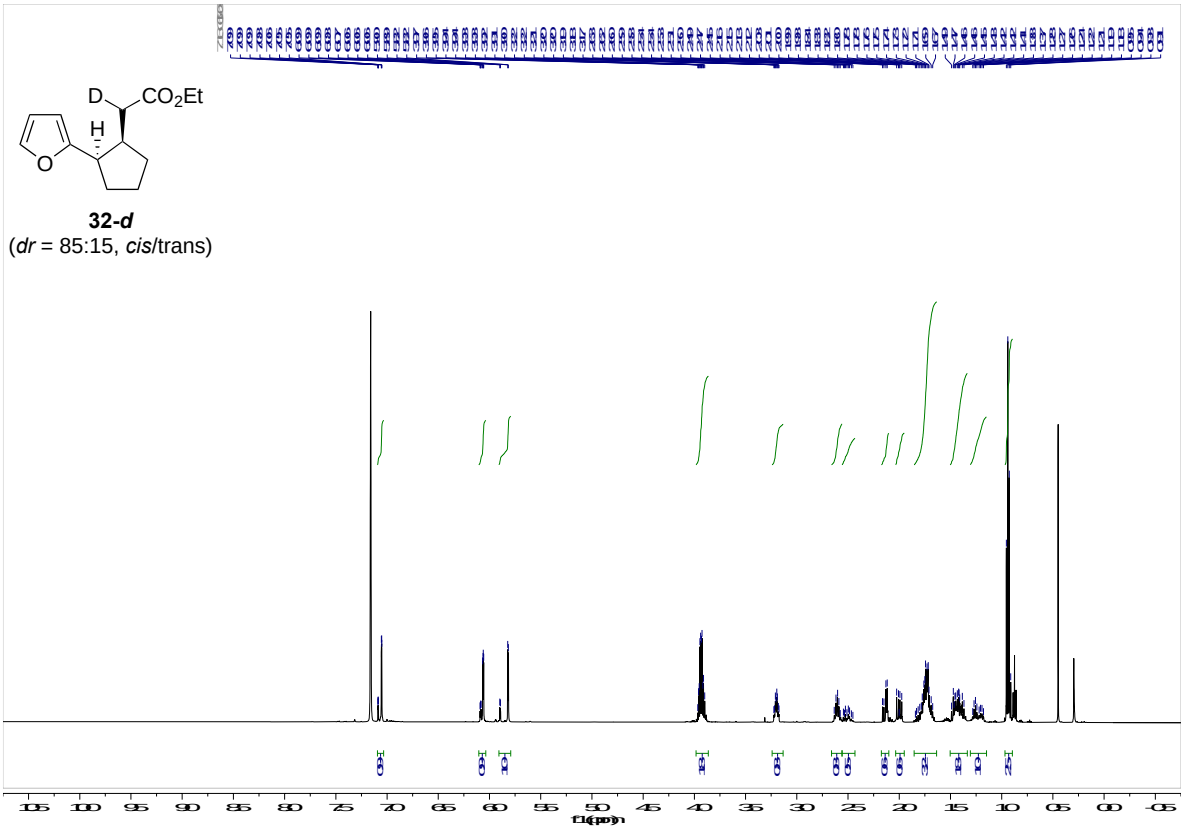

32-*d*
(*dr* = 85:15, *cis*/trans)

^{13}C NMR (126 MHz, C_6D_6)

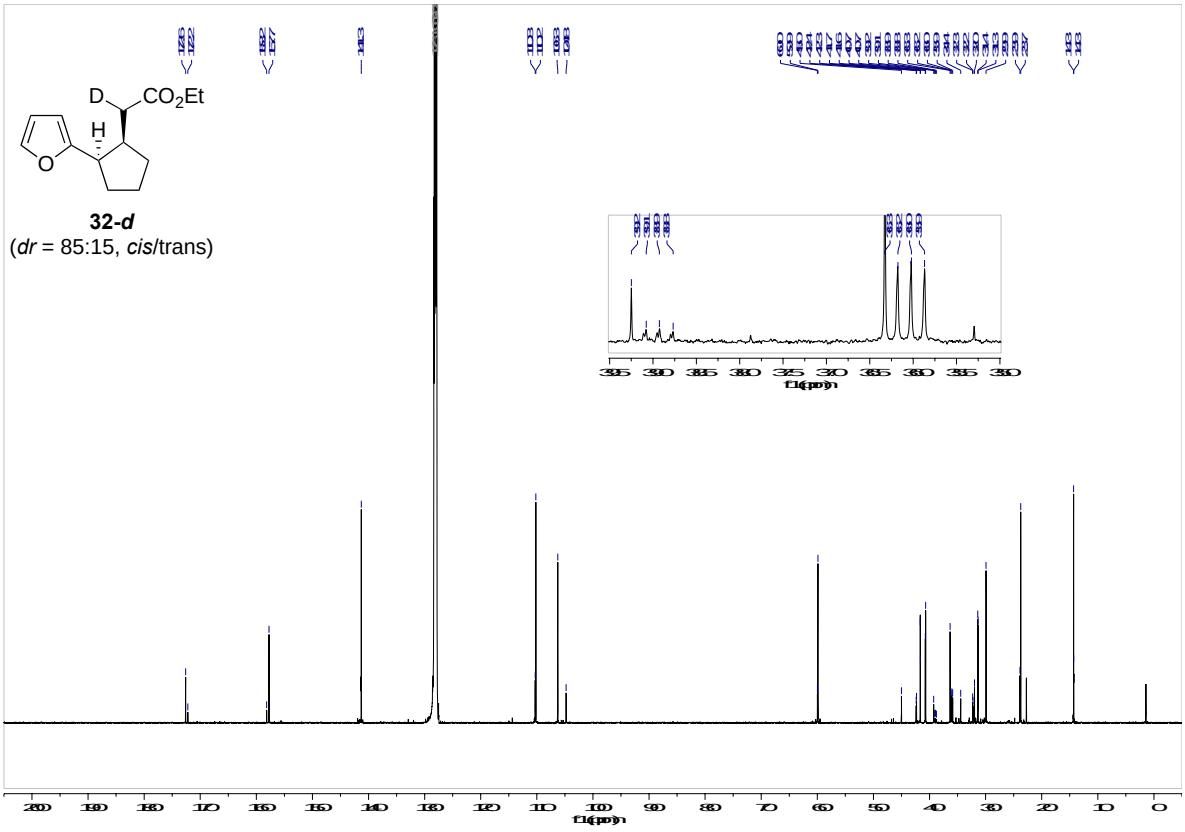

32-*d*
(*dr* = 85:15, *cis*/trans)

^{2}H NMR (92 MHz, C_6H_6 spiked with C_6D_6)

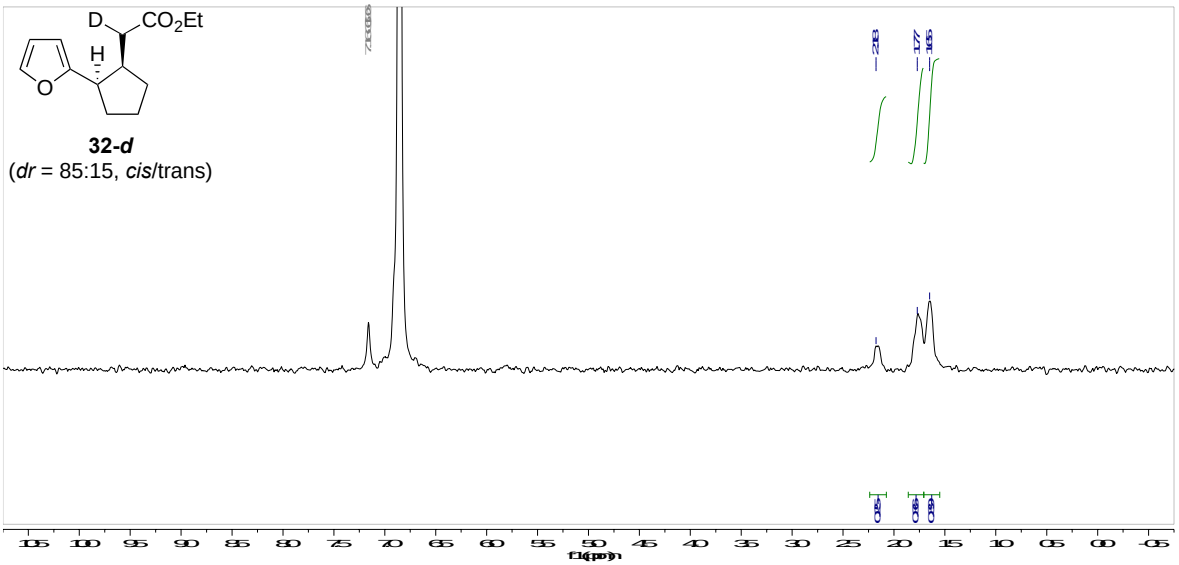

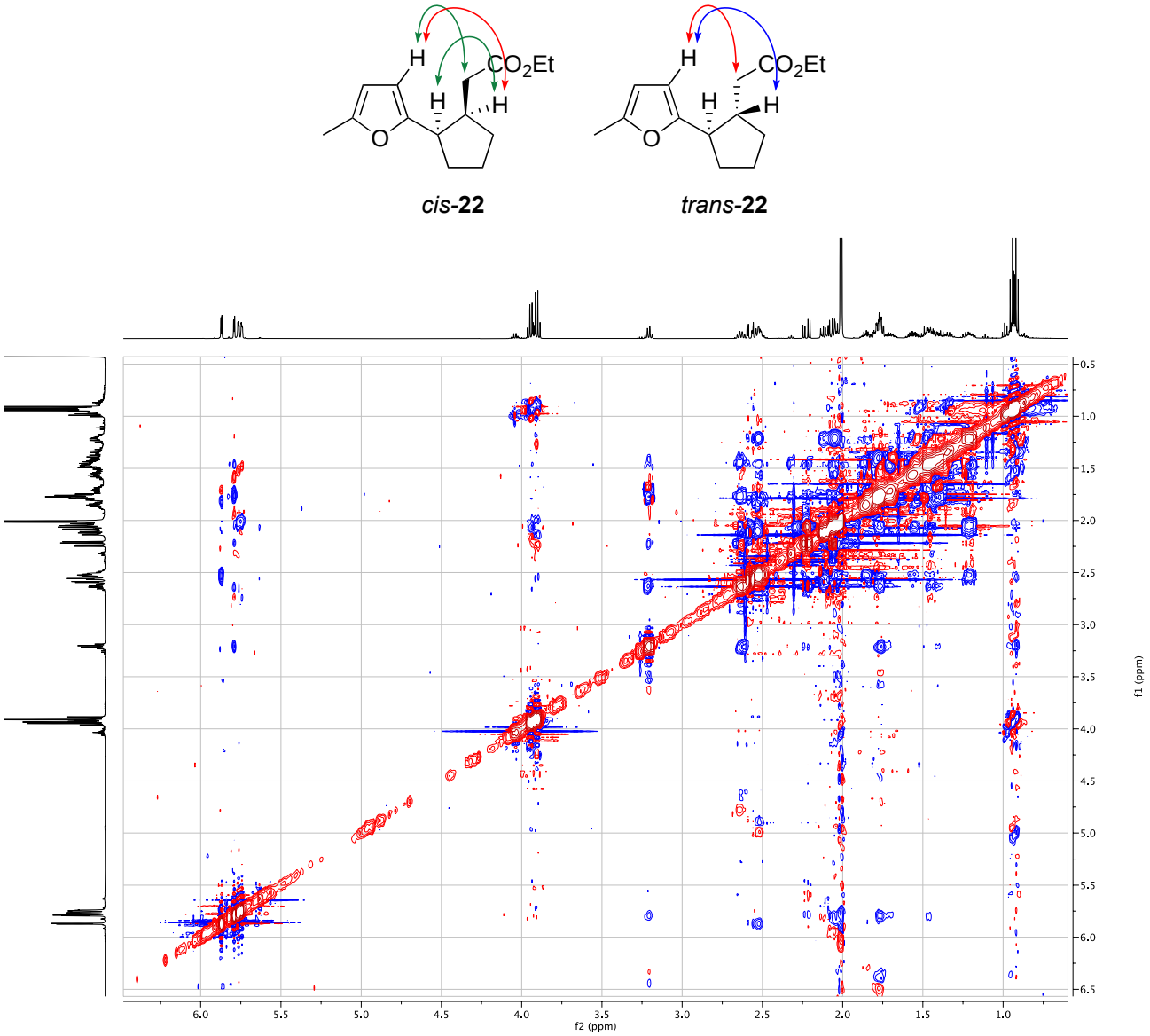

Figure S1 ^{1}H–^{1}H NOESY (500 MHz, C_6D_6) spectrum of compound **22** (*dr* = 52:48, *trans/cis*) from radical cyclisation. Green arrows indicate observed correlations; red arrows indicate those not observed; blue arrow is an ambiguous correlation.

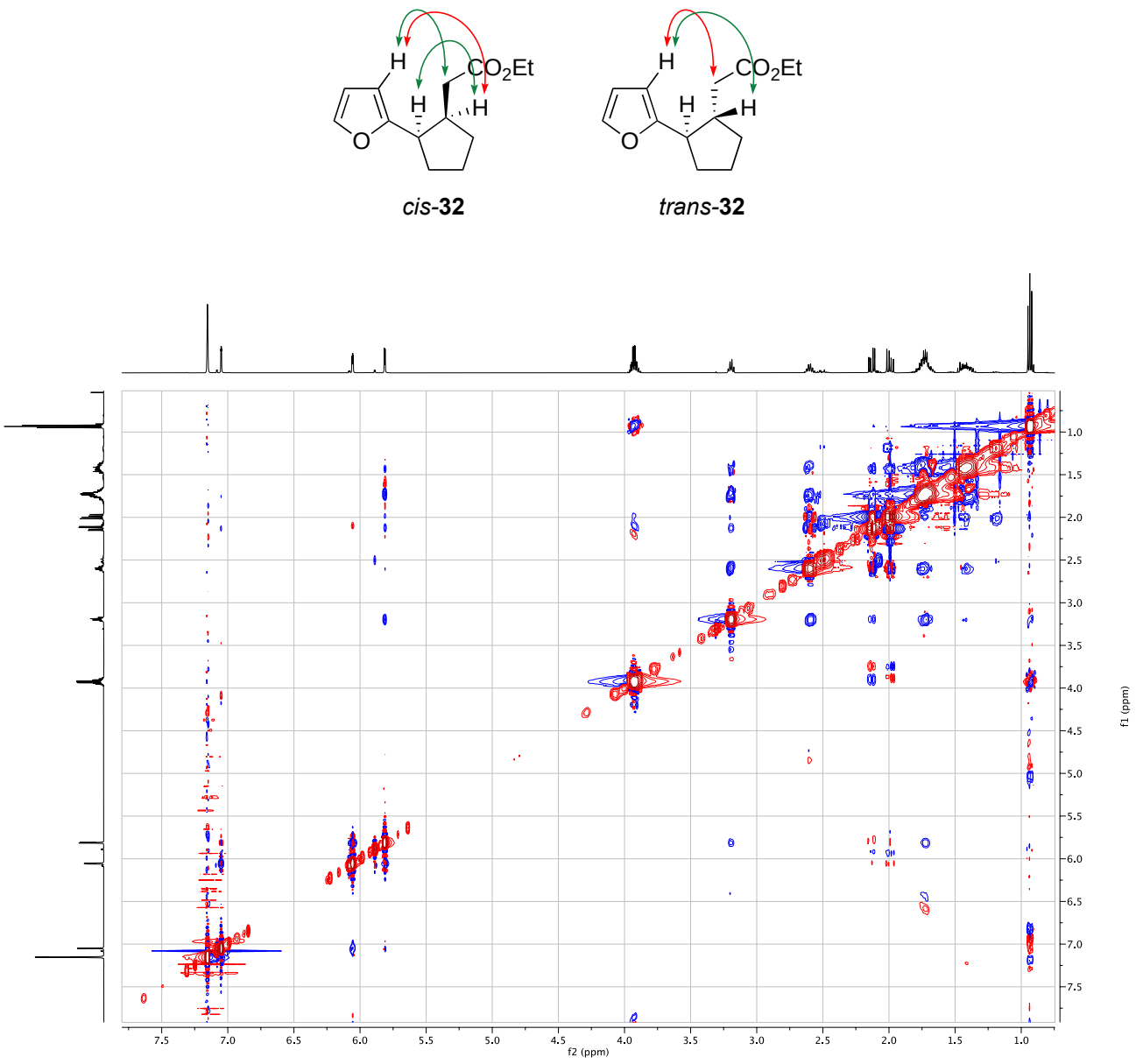

Figure S2 ^{1}H–^{1}H NOESY (500 MHz, C_6D_6) spectrum of compound **32** (*dr* = 90:10, *cis/trans*) prepared by hydrogenation. Green arrows indicate observed correlations; red arrows indicate those not observed.

DFT calculations

*Energy calculations for trans- and cis-**22'***

(a) A conformer distribution was obtained within *Spartan'20* using molecular mechanics (MMFF, MonteCarlo) to generate 38 conformations for *trans*-**22'** and 24 for *cis*-**22'**; the methyl ester was used here to keep the number of conformations to a manageable level.
(b) The low-lying conformations, representing ~95% of the conformational space, were retained: 17 for *trans*-**22'**, 13 for *cis*-**22'**.
(c) DFT (B3LYP/6-31G*) equilibrium geometry calculations of the 30 separate conformations were used to obtain a Boltzmann-weighted average energy for each diastereomer leading to the values presented in Figure 1 of the main text.

*Transition state calculations for the cyclisation of methyl (E)-7-(2-furyl)hept-2-enoate (7-yl radical) (**S6**)*

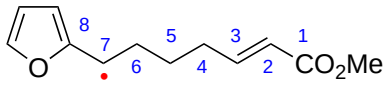

S6

(a) Transition states were computed within *Spartan'20* for the cyclisation of 6-hexenyl radical in both *anti* ('chair') and *gauche* ('boat') conformations as defined in Table 1 of the main text.
(b) These were then used to build the substituted radical **S6** in *anti* and *gauche* conformations, each configured to lead to either *cis* or *trans* disubstituted cylopentane.
(c) For each of the four so-generated transition state approximations, a conformer distribution was obtained (MMFF, MonteCarlo) with the hexenyl radical core frozen (Table S1).
(d) DFT (B3LYP/6-31G*) equilibrium geometry calculations of the 28 separate radical conformations, with the cores unfrozen, were used to obtain an energy-weighted conformer distribution within each parent.
(e) In all cases, based on the Boltzmann weightings, just one or two low-lying conformations accounted for 83–90% of the conformational space; these were selected for DFT (B3LYP/6-31G*) transition state calculations with all constraints removed, leading to the energies presented in Table 1 of the main text.

Table S1. Numbers of conformations taken through each stage of the transition state calculations.

Conformation	MMFF conformers	Number selected for TS calcns
anti-cis	4	1 (83%)
anti-trans	5	2 (83%)
gauche-cis	9	1 (86%)
gauche-trans	10	2 (90%)

